Determining Bearing Resistance of Cantilever Sheet Piles BDV31-977-90

Project Manager
Juan Castellanos, PE

Principal Investigator:
Xiaoyu Song, Associate Professor, Ph.D.
Researchers:
Amirata Taghavi, PhD.
Shashank Menon, Ph.D.
Kaiqi Wang, Ph.D.
Zhe Zhang, PhD Student

Date
08/11/2022

Department of Civil and Coastal Engineering
University of Florida

FDOT

Outline

- Project description
- Background
- Objectives
- Task 1: Literature Review
- Task 2: Numerical Modeling
- Task 3: Centrifuge Testing
- Task 4: Validation and Design Equations
- Summary & Future Work
- Acknowledgement

Project description

Determine the axial load capacity of cantilever sheet pile wall considering both end bearing and side friction

- Test a variety of site conditions, structural properties and loading
- Develop practical design method for axially loaded sheet pile foundations
- Propose practical protocol to conduct axial load tests of sheet piles in the field

Project Benefits

I. Qualitative:

Simple design equations for sheet pile walls in sandy soil under combined axial/lateral loading

II. Quantitative:

Potential cost savings by eliminating need for sperate deep foundations

Background

- The current FDOT practice requires discrete deep foundation (piles or drilled shafts) for vertical bearing purposes.

- Using sheet piles to support both vertical bridge loads and lateral earth loads. However, this concept has not survived final design due to the inability to confirm the capacity of these elements in the field and accept them as bearing piles.

- For end bents of small bridges, there is a potential for realizing savings if we can verify the axial resistance of the sheet piling for vertical bearing purposes.

- This would also relieve the complications that arise in construction when driving piles and sheet piles in close proximity.

Background (cont'ed): Uncertainties and Issues

- Evaluation of side friction and end bearing resistance by conventional pile design approaches
- Assessment of soil-sheet pile interaction under combined axial and lateral loading
- Influence of pile head fixity on the bending moments and turnover
- Determination of the bearing capacity of axially loaded sheet piles through standardized practical field testing protocols

Objectives

I. Quantify the bearing capacity of permanent steel sheet pile walls
II. Evaluate both the friction and bearing components
III. Develop practical recommendations for designers to estimate the bearing capacity of steel sheet pile walls
IV. Develop practical methods to determine and verify the bearing capacity in the field

Research Tasks

Task 1 - Literature Review and Information Collection

Task 2 - Numerical Modeling

Task 3 - Centrifuge Testing of Model

Task 4 - Numerical Validation & Design Equations

Task 1 – Literature review (numerical)

- Shiau and Smith (2013) reported that using finite difference model of cantilever sheet pile wall is more accurate to the analytical solution when compared to the limit equilibrium method solutions

- Al-Baghdadi, et al. (2017) conducted 3D finite element simulations of screw piles under combined axial and lateral loading.

- Karthigeyan et al. (2006,2007) conducted 3D finite element simulations of sheet piles under combined axial and lateral loading.

- Azzam and Elwakil (2017) used a plane strain, two-dimensional finite element program to simulate the piled retaining wall under axial load using. They reported that surcharge loading near the pile led to significant decrease in ultimate axial loading capacity.

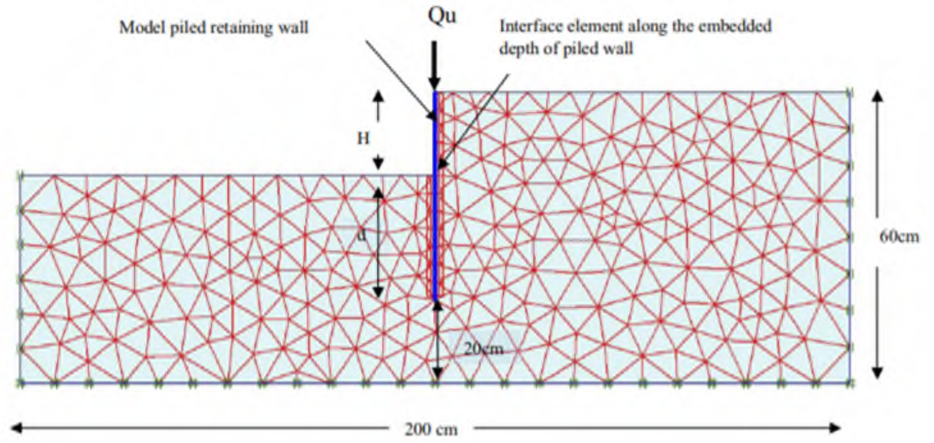

Figure 2: Geometry, generated mesh, and boundary conditions of sheet pile model (Azzam & Elwakil, 2017)

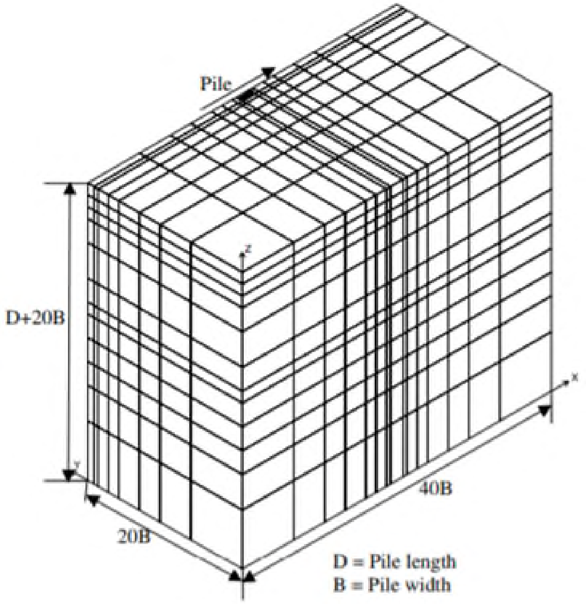

Figure 3: Typical mesh for three-dimensional finite element analyses (Karthigeyan et al., 2006)

Task 1 – Literature review (Lab testing)

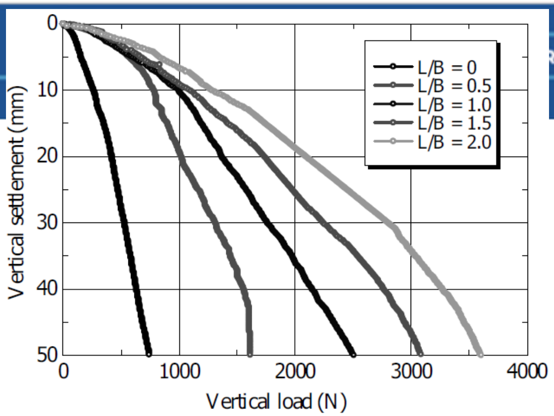

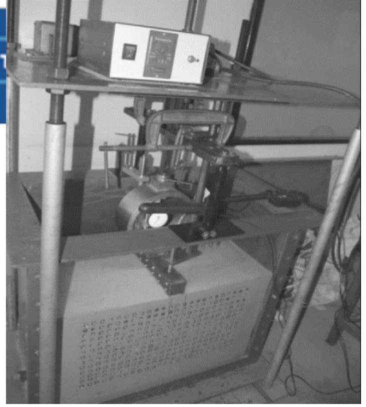

a. Load testing set up	b. Load-settlement curves for the foundation systems

Figure 4: Load testing of shallow foundations enclosed by sheet piles (Punrattanasin et al., 2009)

- Punrattanasin et al . (2009) detailed how to prepare soil for different relative density using pluviation.

- Azzam and Elwakil (2017) identified critical factors affecting axial capacity of sheet piles: <u>penetration depth, pile stiffness, and sand relative density</u>

Figure 5: Pictures of the sheet pile under axial loading (Azzam & Elwakil, 2017)

Task 1 – Literature review (Centrifuge testing)

- Madabhushi and Chandrasekaran (2008) demonstrated that a centrifuge soil-pile system could accurately capture commonly observed failure modes in the field. Their <u>test and instrumentation set-up informed our geo-centrifuge test.</u>

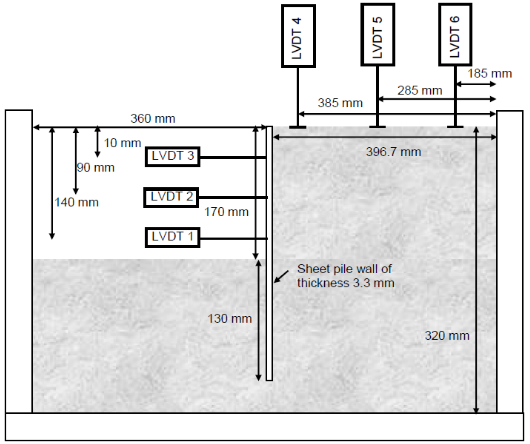

Figure 7: Schematic diagram of the cross-section of the centrifuge model (Madabhushi & Chandrasekaran, 2008)

- Bolton and Powrie (1987,1988) conducted centrifuge model tests to form the basis of research into the soil-structure interaction behavior following the excavation of soil

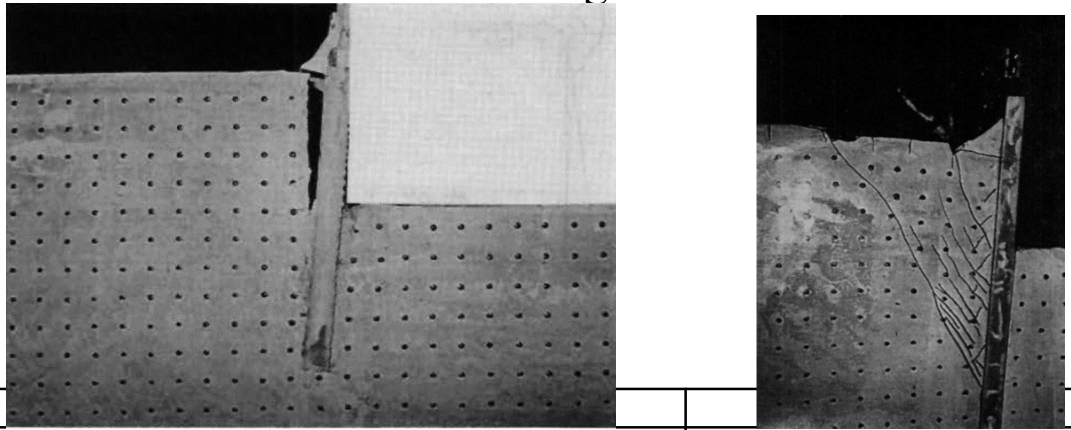

(a) Flooded tension crack failure in the wall with shallow penetration	(b) Post-flight view of the wall with deeper penetration

Figure 6: Observed modes of collapse (Bolton & Powrie, 1987)

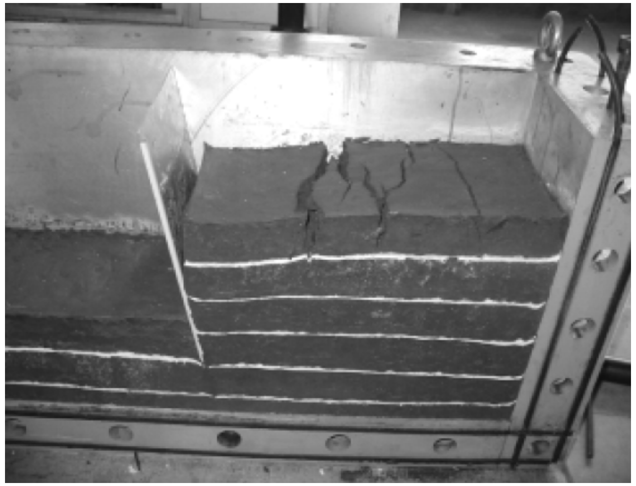

Figure 8: View of the model after the test showing the rotation of the sheet pile wall

Task 1 – Literature review (Field testing)

- Sylvain et al. (2017) conducted static axial load tests on a pair of PZ 27 sheet piles in general accordance with ASTM D1143/D1143M (2013).

- Doubrovsky and Meshcheryakov (2015) conducted press-in full-scale tests to study the dependencies between the applied forces and the developed friction in the interlocks

- S. Taenaka et al. (2016a) tested closed-end sheet piles to enhance load capacity through plugging

a. Photo of the test pile and the reaction frame	b. Photo of the test H-pile prior to static load test

Figure 5: Photos of the test setup for the axial load test (Sylvain et al., 2017)

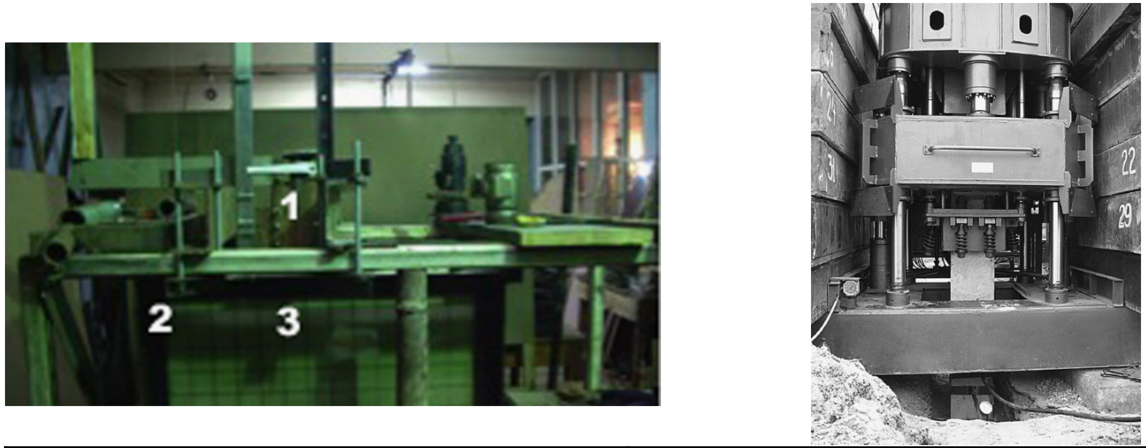

a. Press-in piling machine SO-450	b. Laboratory test set-up showing sheet pile elements (1), soil container (2), and glass walls (3)

Figure 9: Setups for investigating interlock friction of sheet piles (Doubrovsky & Meshcheryakov, 2015)

Insights – Numerical modeling

- Details on how to develop the numerical model (elements, interface properties, material model, etc.)
- Larger penetration depth increases limit of maximum bending moment
- Three-dimensional simulations of sheet pile wall should be conducted to better model vertical bearing capacity of sheet piles

Insights – Physical testing

- The key factors affecting axial capacity are soil density, pile stiffness, penetration depth
- The pile would have to be driven while the centrifuge was inflight
- Geo-centrifuges could accurately reproduce observed failure modes
- Constant rate penetration was preferable to maintained load penetration

Task 2 - Simulation Scenarios

1. Effect of penetration depth and unsupported length
2. Effect of sheet pile wall stiffness
3. Effect of sand relative density and layering
4. Effect of the sheet pile head fixity
5. Effect of surcharge load

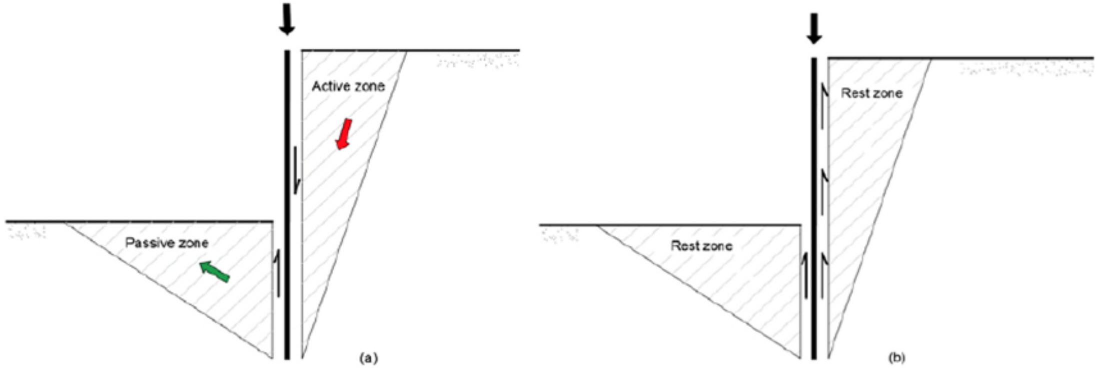

Figure 15: Skin friction developed in the axially loaded sheet pile: (a) free head conditions; and (b) fixed head conditions.

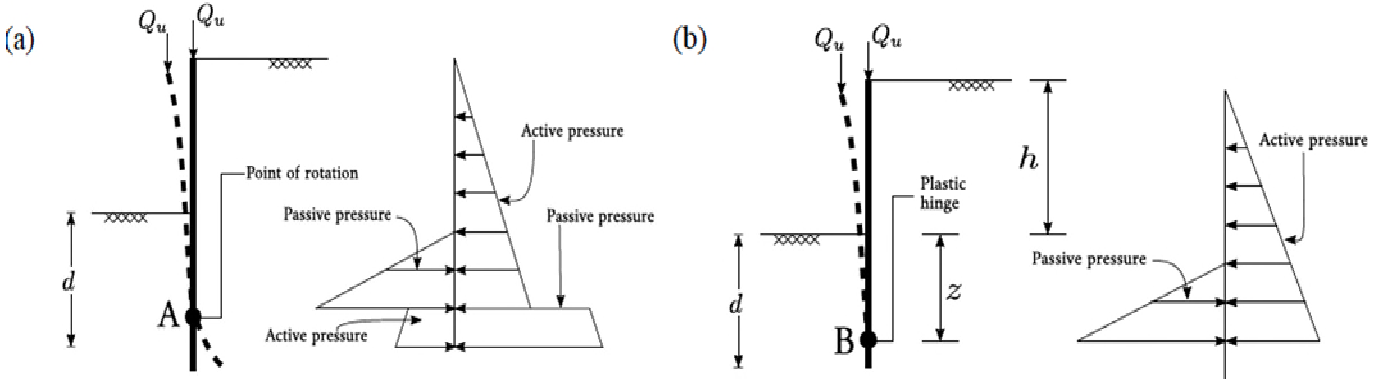

Figure 14: Failure modes of cantilever sheet pile walls:
(a) Failure due to rotation about point A and
(b) Failures due to the formation of a plastic hinge at point B.

Task 2 – Simulation scenarios

Parameter	No. of Cases	No. of Pile Depths Considered	Total No. of Scenarios
Density	3	10 (15 – 22.5 ft)	30
Internal friction	3	10 (15 – 22.5 ft)	30
Tip Resistance	2	10 (15 – 22.5 ft)	20
Head Boundary	2	10 (15 – 22.5 ft)	20
Surcharge	2	10 (15 – 22.5 ft)	20

- Uniform sand profile for 10 embedment ratios in 3 different sands (density and friction angle)
- For tip resistance: the tip of the pile wall is embedded in very dense sand overlaid by different sand layer
- Head boundary conditions are studied by comparing effects of a fixed and free head condition.

Task 2 - Nonlinear FE Model

Table 1. Material properties used in the finite element simulations

Parameter	Sheet pile	Very dense sand	Dense sand	Loose sand	Interface elements
Material model	Elastic	Mohr-Coulomb	Mohr-Coulomb	Mohr-Coulomb	Mohr-Coulomb
Young's modulus	438594.12 ksf	2360.1 ksf	2006.1 ksf	1705.2 ksf	/
Cohesion	-	0	0	0	/
Poisson ratio	0.25	0.3	0.3	0.3	/
Friction angle	-	35	32	27	/

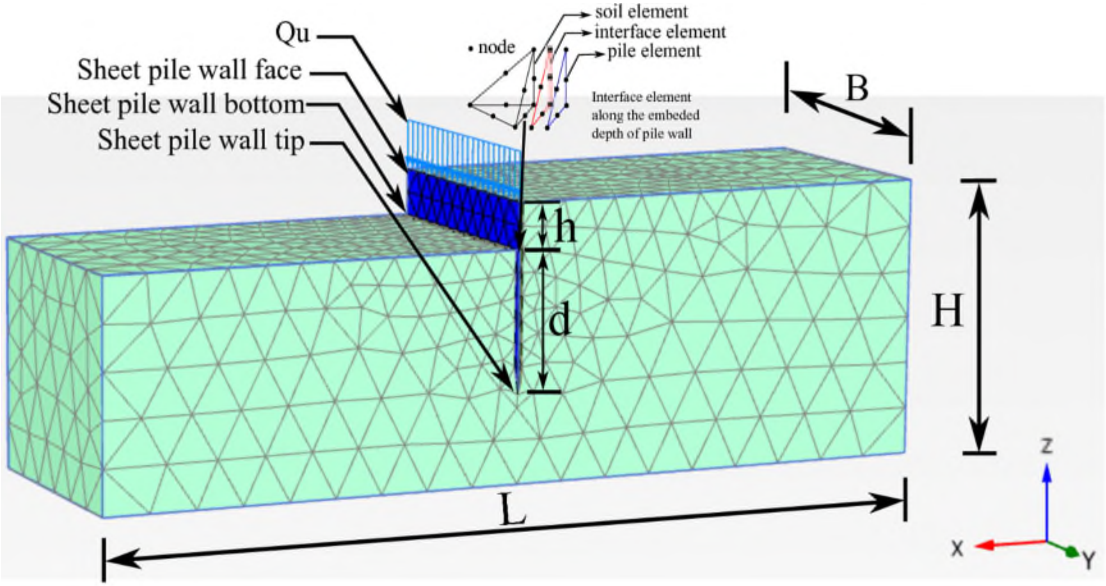

Figure 10. Finite element model for the sheet pile wall

- Sand: Elastic-plastic Mohr-Coulomb model by continuum elements (tetrahedrons)
- Sheet pile wall: an elastic model by a structural element (plates)
- The interface: Elastic-plastic Mohr-Coulomb model

Task 2 - Embedment

- Effect of penetration depth and unsupported length

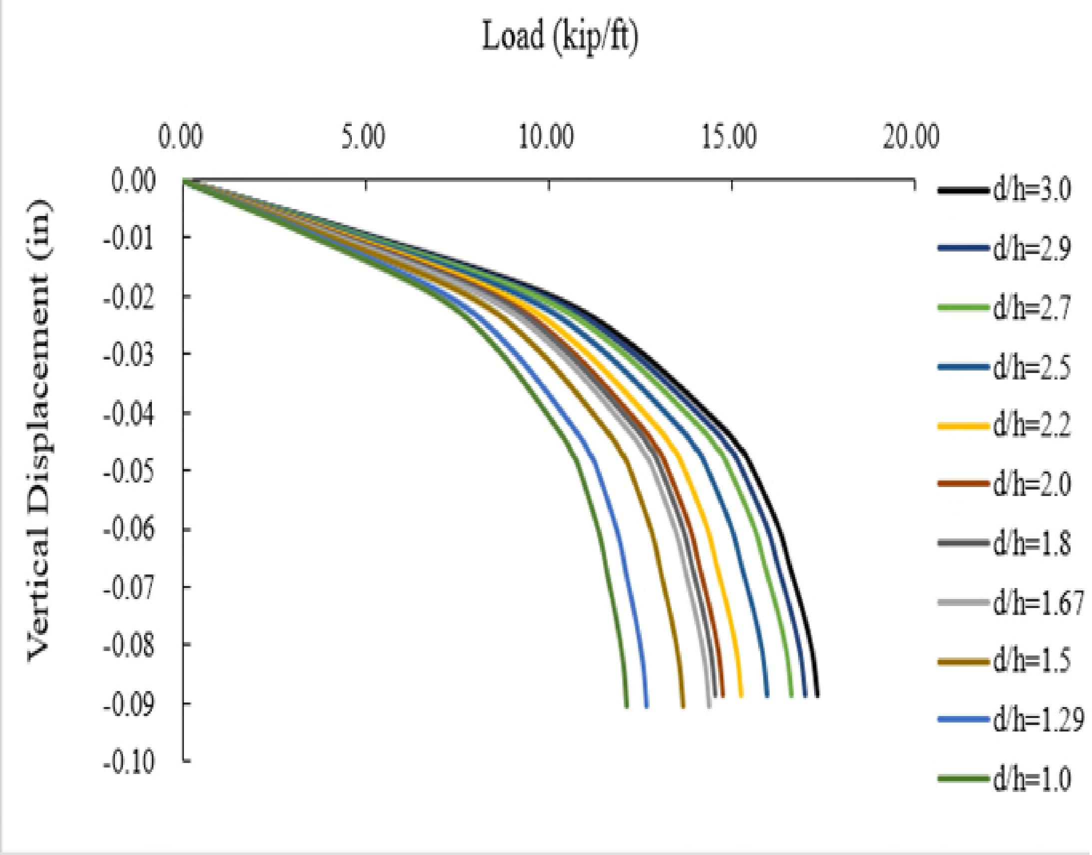

Figure 11. Load versus vertical displacement curve of very dense sand for different ratio of d/h

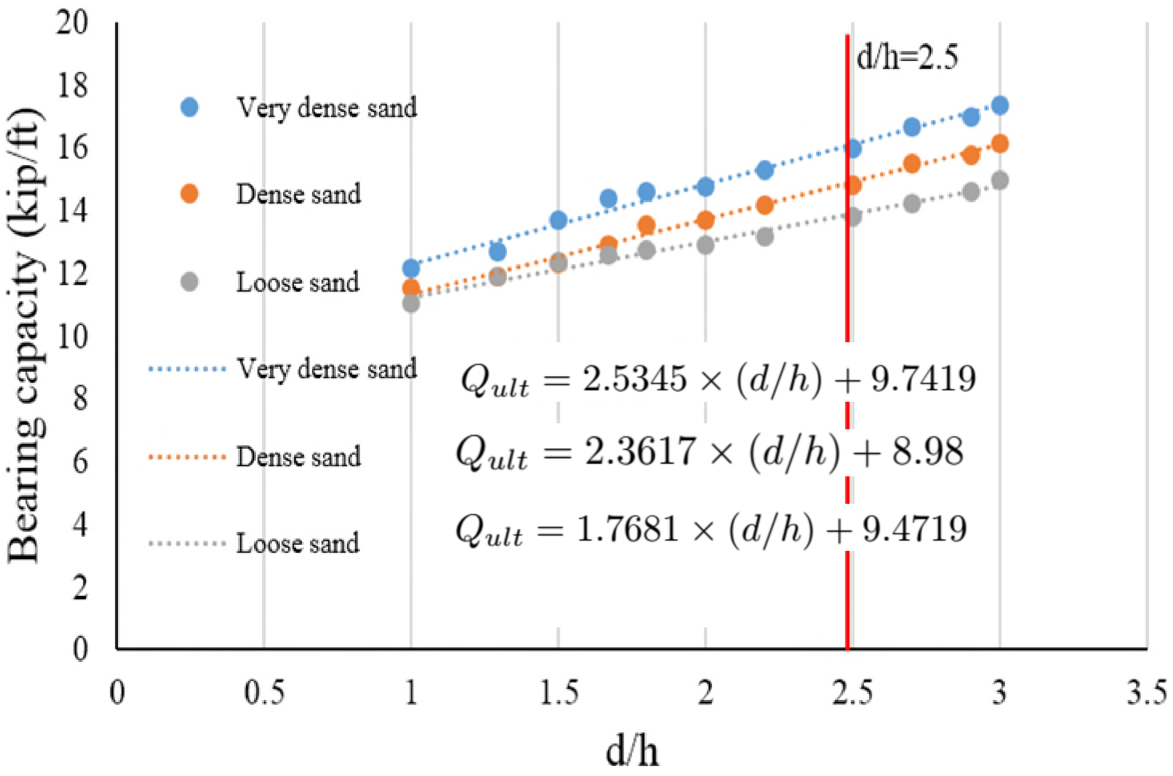

Figure 12. Relationship between the bearing capacity and ratio of d/h

Task 2 – Pile Stiffness

- Effect of sheet pile wall stiffness

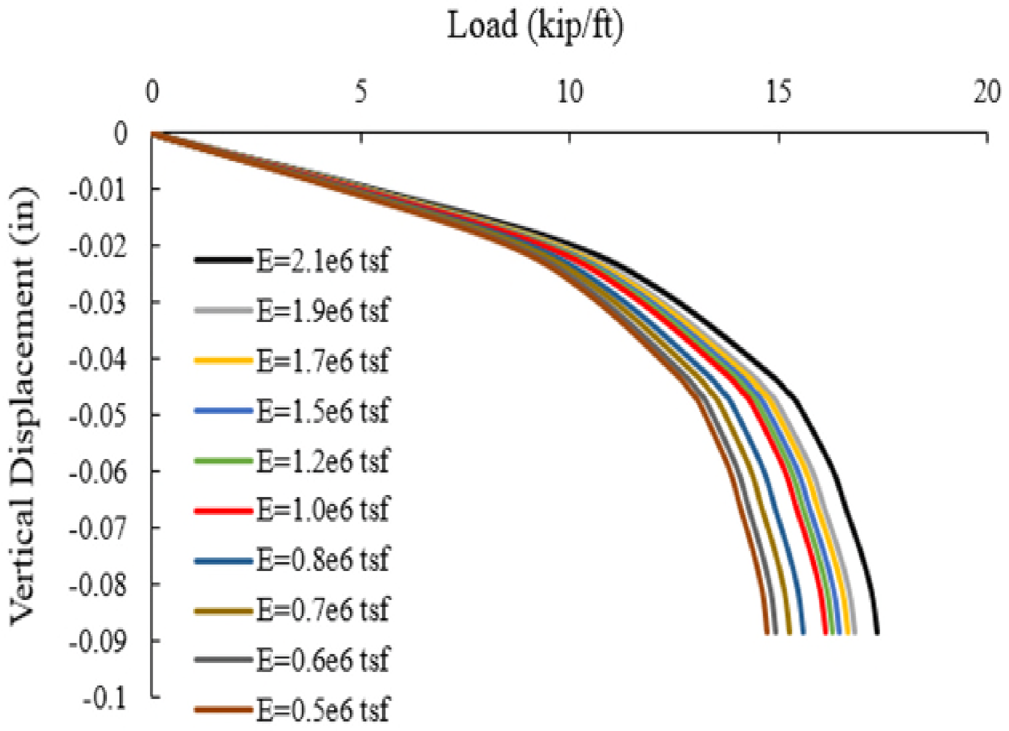

Figure 13. Load versus displacement curve for different Young's modulus of sheet piles for very dense sand.

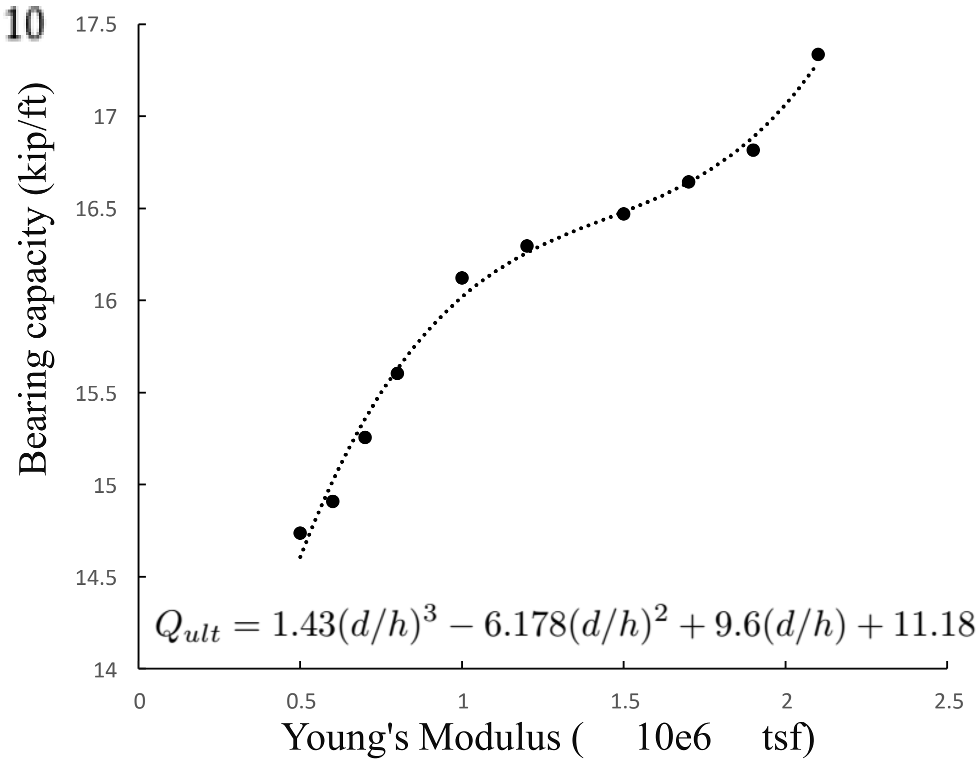

Figure 14. Relationship between the bearing capacity and stiffness of steel

Task 2 – Head fixity

- Effect of the sheet pile head fixity

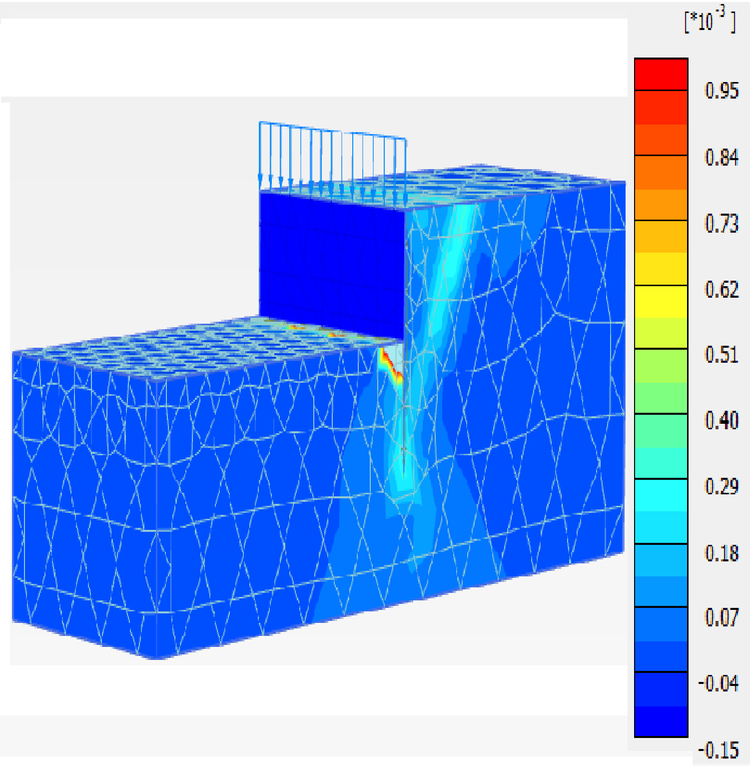

Figure 15. Contour of plastic shear strain for free head condition at d/h = 1

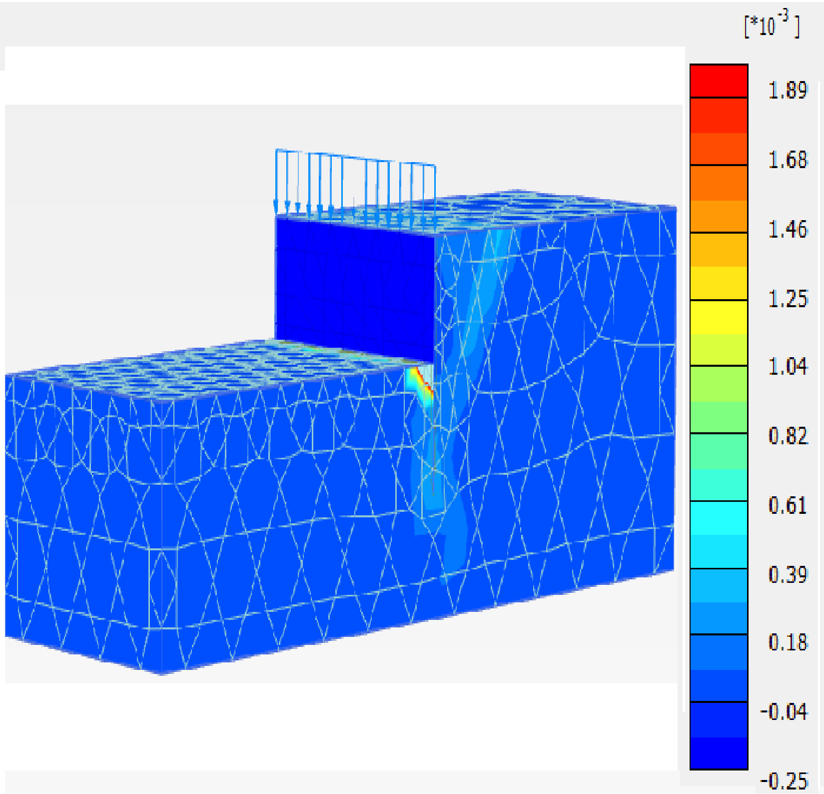

Figure 16. Contour of plastic shear strain for fixed head condition at d/h = 1

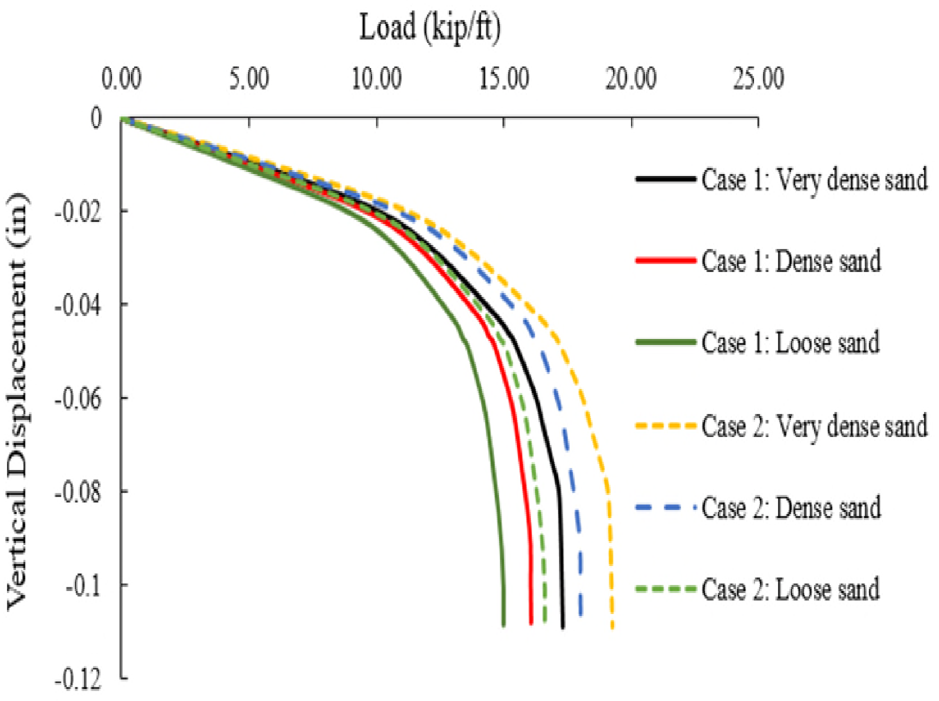

Figure 17. Load versus vertical displacement curve of different density sand at ratio of d/h=1: Case 1 for the free head condition and Case 2 for the fixed head condition

Task 2 – Tip resistance

- Effect of sand relative density and layering

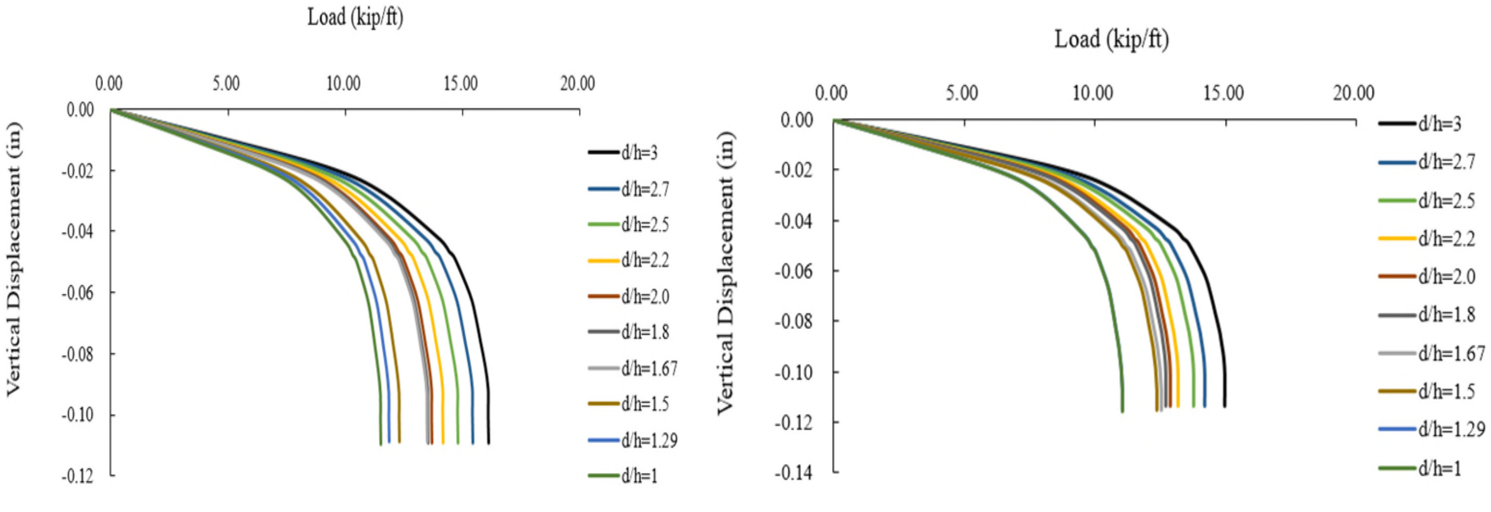

Figure 18. Load versus vertical displacement curve of top dense sand (left) and top loose sand layer (right) for different ratio of d/h

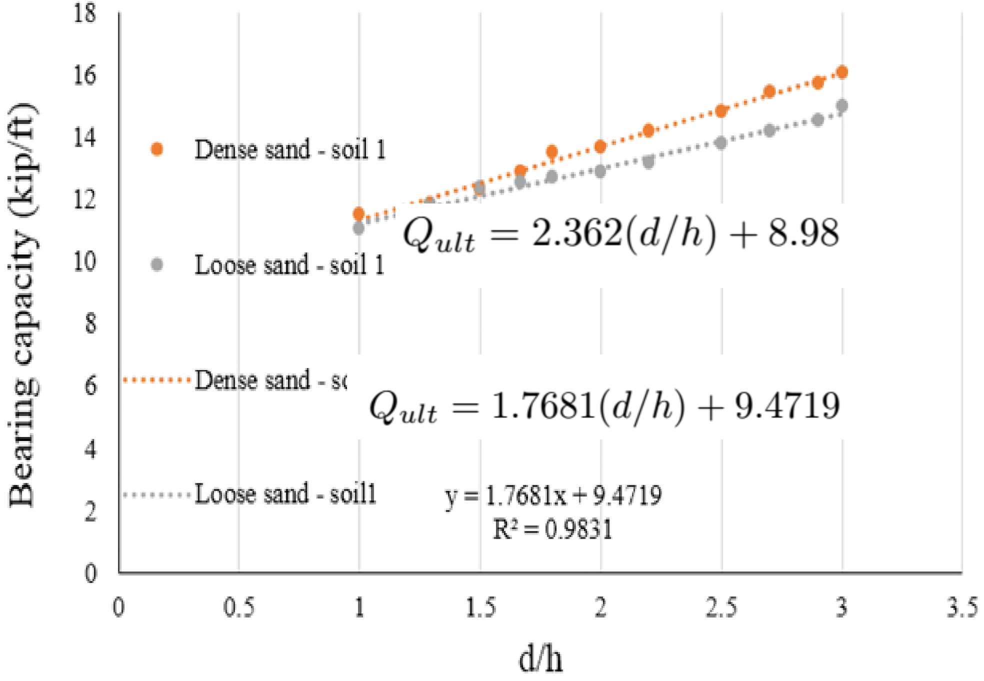

Figure 19. Relationship between the bearing capacity and ratio of d/h for two layers

Task 2 – Tip resistance

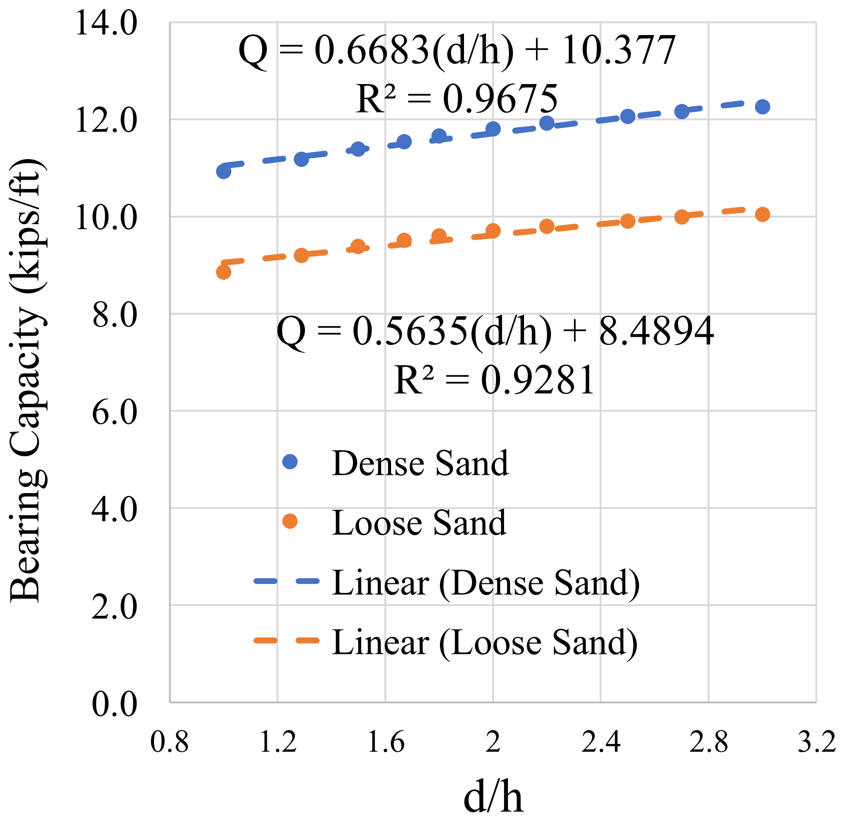

Figure 20 Plot of bearing capacity over the embedment ratio for layered sand profiles

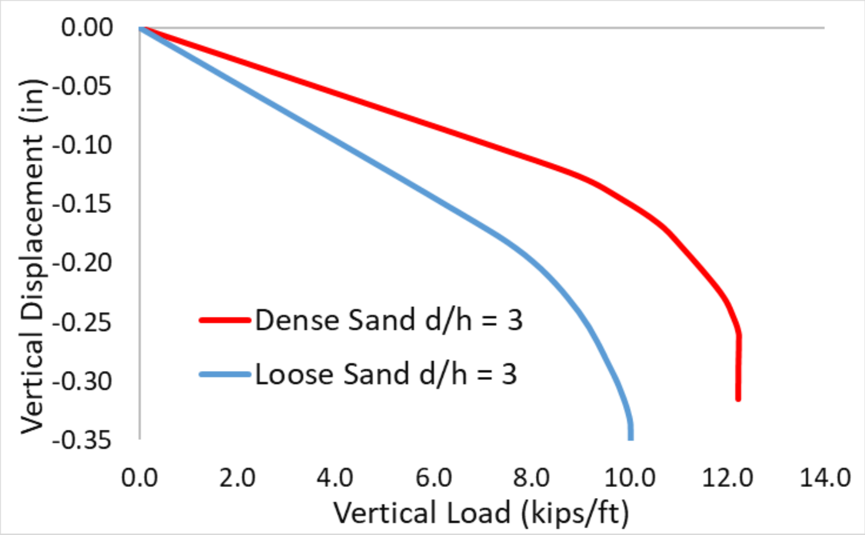

Figure 21 Vertical load over displacement for d/h = 3.0

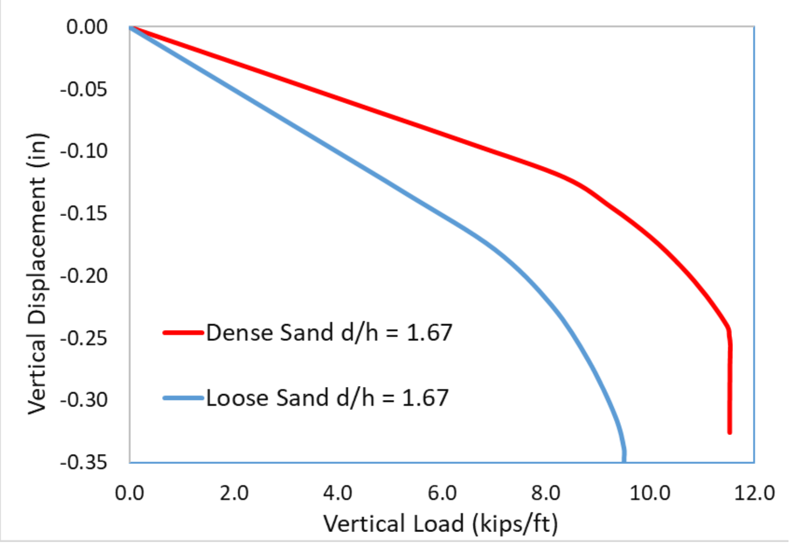

Figure 22 Vertical load over displacement for d/h = 1.67

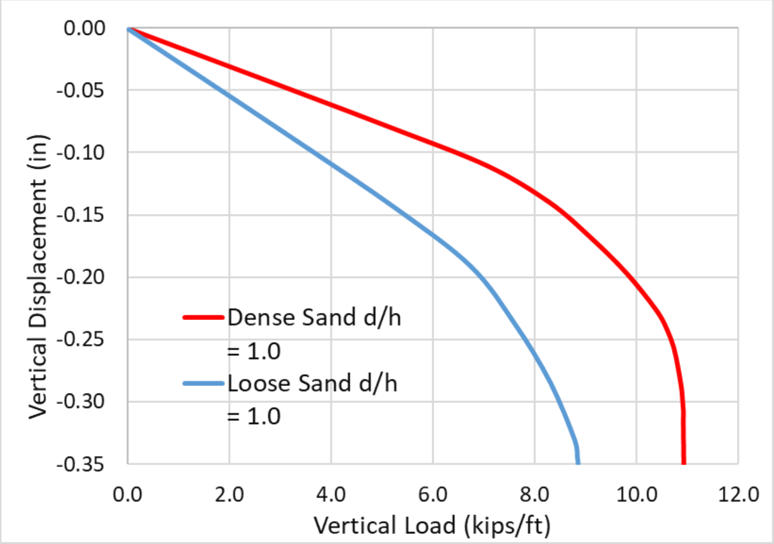

Figure 23 Vertical load over displacement for d/h = 1.0

Task 3 – Centrifuge testing

- Understand the behavior of axially loaded sheet pile walls through investigating the effects of
  - *- sand relative density and soil layering,*
  - *- sheet pile wall penetration depth,*
  - *- sheet pile wall head boundary conditions,*
  - *- rate effects during load testing, and*
  - *- sheet pile wall stiffness*
- Validate numerical models

Task 3 – Test setup

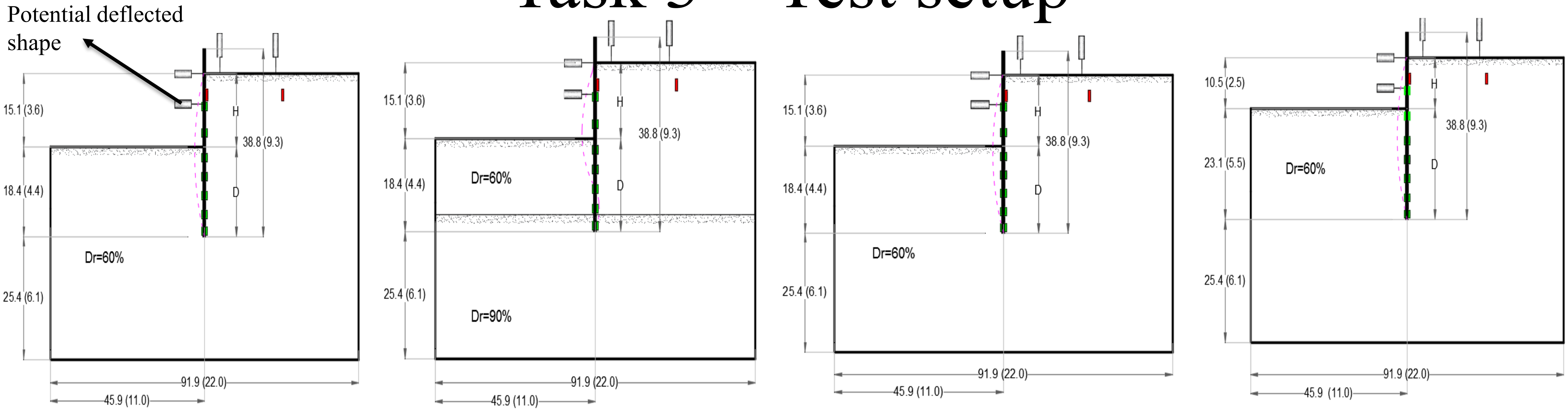

Figure 24: The centrifuge model setup. All dimensions in feet at prototype-scale (and inches in model-scale)

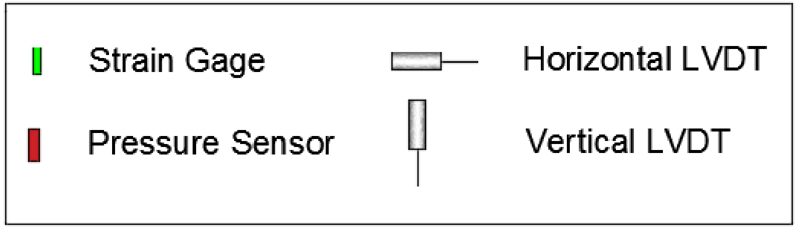

I) Axial load transferring mechanism

II) Penetration depth and unsupported length

III) Sheet pile head boundary conditions

IV) Axial load testing of sheet pile abutments: static and quasi-static

V) Sheet pile stiffness

Task 3 – Test setup

- Centrifuge test set-up

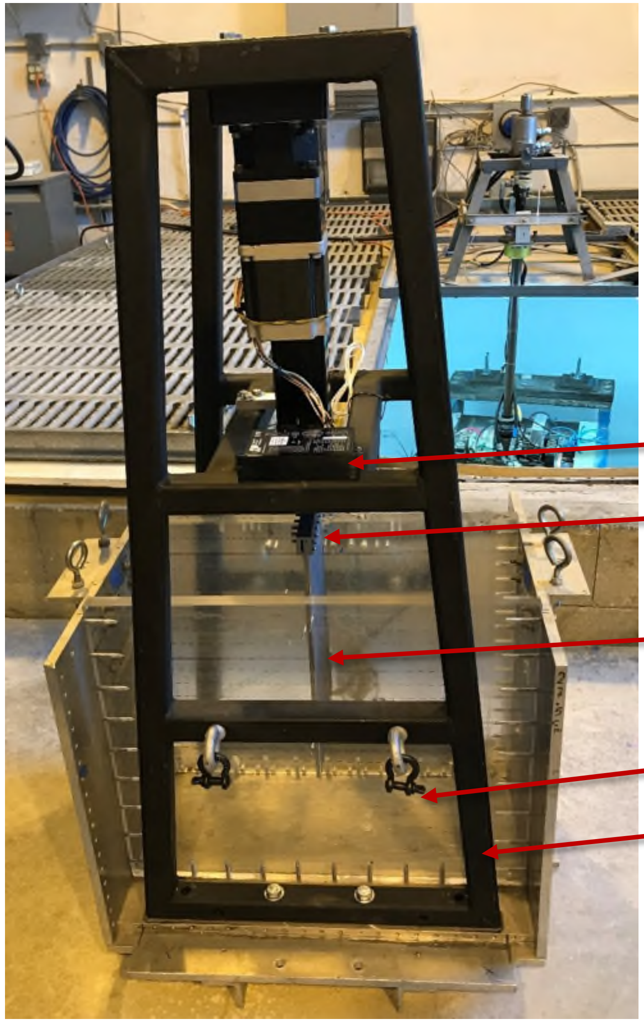

Stepper Motor
Actuator
Feedback LP
Custom-made
Load Cell
Controller
Helmet
Sheet Pile
Container
Frame

Task 3 – Sheet pile properties

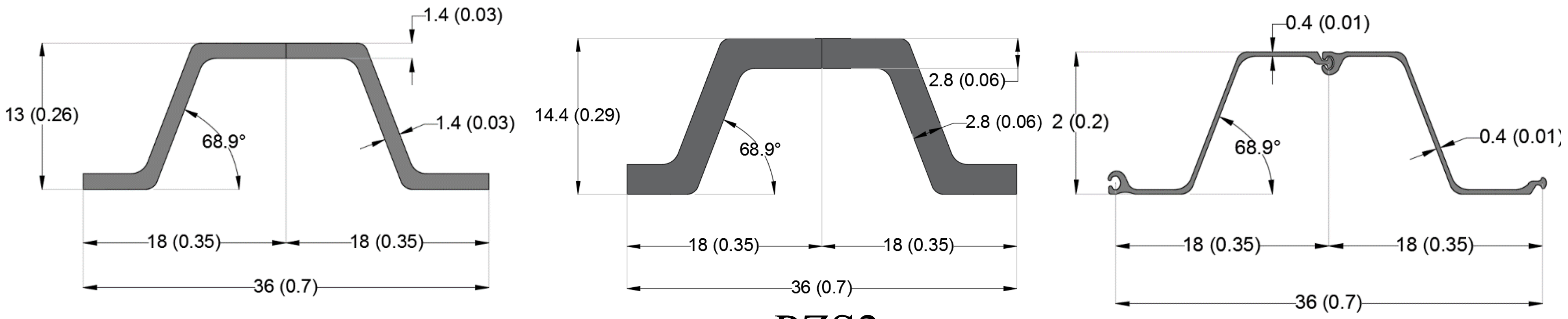

PZS1 PZS2 PZ27

Figure 25: Sheet pile wall section with dimensions in inches at prototype-scale (and in model-scale)

Sheet pile section dimensions and properties

	Model-scale (1 g)		Prototype-scale (50 g)		PZ section
Section	PZS1	PZS2	PZS1	PZS2	PZ27
Width (in)	0.7	0.7	36	36	36
Height (in)	0.26	0.29	13	14.4	12
Flange thickness (in)	0.03	0.06	1.4	2.8	0.4
Web thickness (in)	0.03	0.06	1.4	2.8	0.4
Cross Sectional Area, A (in^2/ft)	0.03	0.06	72	144.4	24.2
Perimeter, P (in/ft)	0.22	0.23	10.77	11.32	11.83
Moment of inertia, I (in^4/ft)	0.001	0.002	7,369.8	1,5217.4	2,649.8
Material	aluminum	aluminum	aluminum	aluminum	steel
Young's modulus, E (psi)	10^7	10^7	10^7	10^7	2.9×10^7
Bending stiffness, EI ($kips.in^2/ft$)	12	24.7	7.5×10^7	1.5×10^8	7.7×10^7
Axial stiffness, EA (kips/ft)	292.3	586.8	731,164	1,466,341	702,678

Task 3 – Soil properties

Figure 26: **UF centrifuge,** Radius = 1.5 m; Acceleration = 50 g

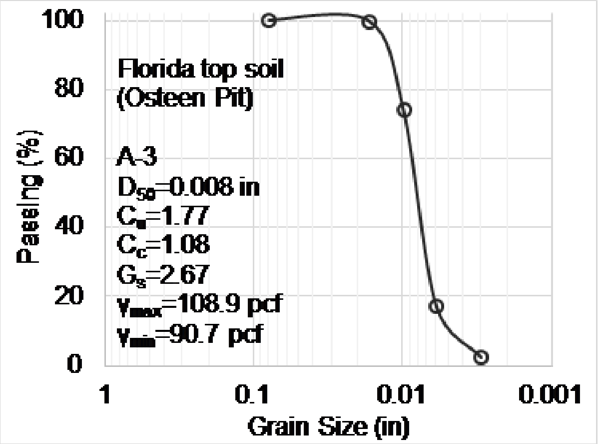

Figure 27 : Target relative densities of FL sand (by pluviation) = 60% and 90%

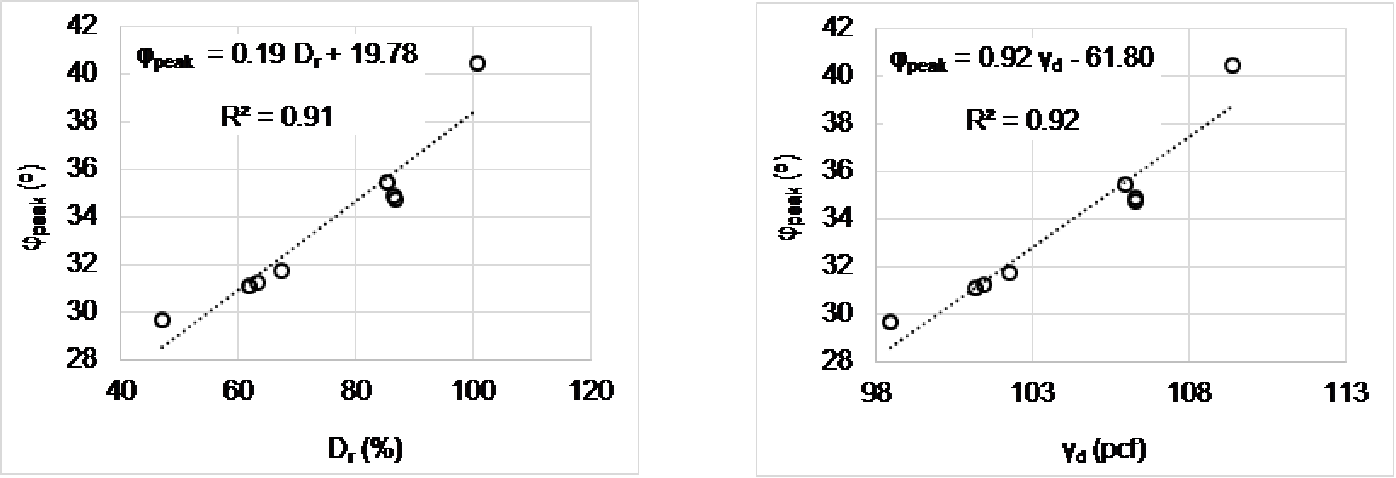

Figure 28: Friction angle over (left) relative density and (right) unit weight

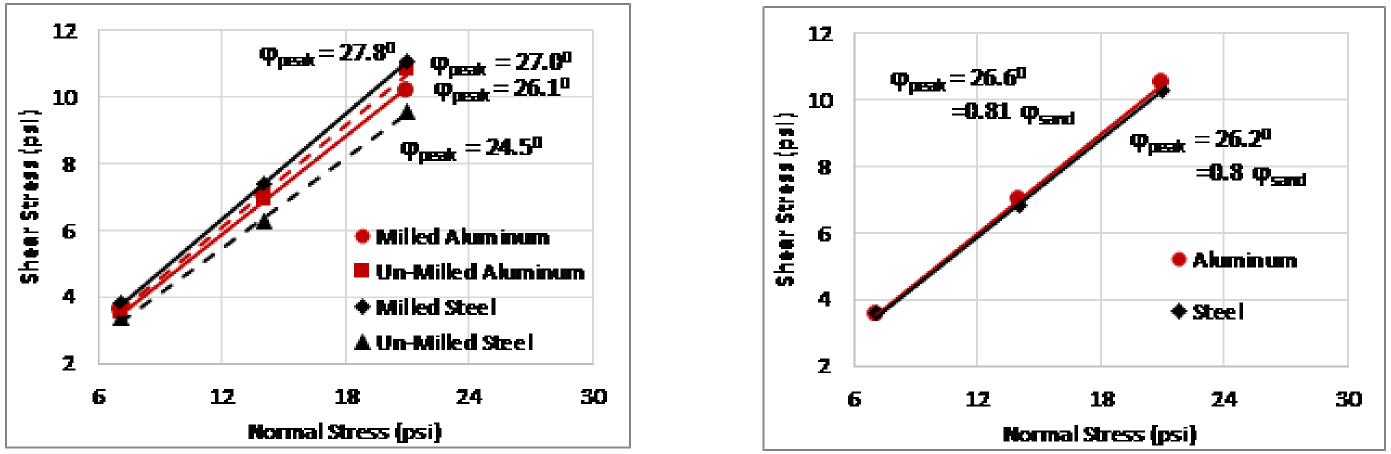

Figure 29: Friction angle at the interface derived from shear box tests

Task 3 - Centrifuge Results

- For uniform layers: pile wall is in medium dense sand with relative density D_r = 63%. (PR1). Scenario represents sheet pile that carries axial load through skin friction

- For layered sand : pile tip is embedded in very dense sand (D_r = 85%) underlaying a medium dense sand. (PR2). This scenario represents tip resistance contributing to the bearing resistance of the pile.

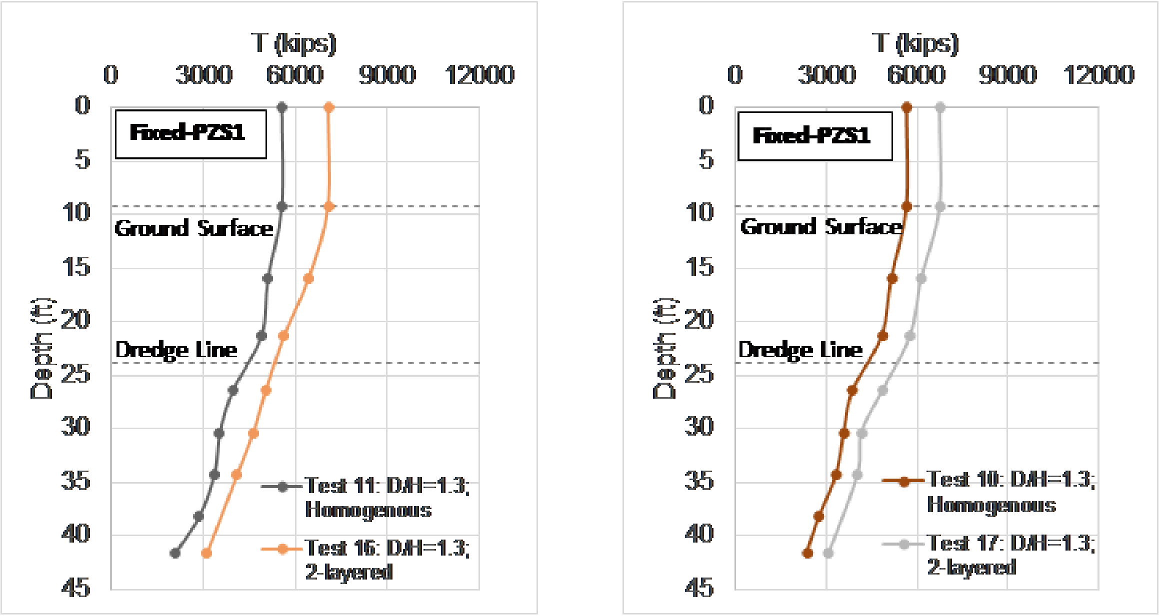

(a) (b)

Figure 30: Increased axial resistance of the sheet pile wall PZS1 in the profile PR2 (tests 16 and 17) compared to that in the profile PR1 (tests 11 and 10) with CRP: (a) CPR=7.87×10^{-4} in/s; and (b) CPR=7.87×10^{-5} in/s for d/h = 1.3

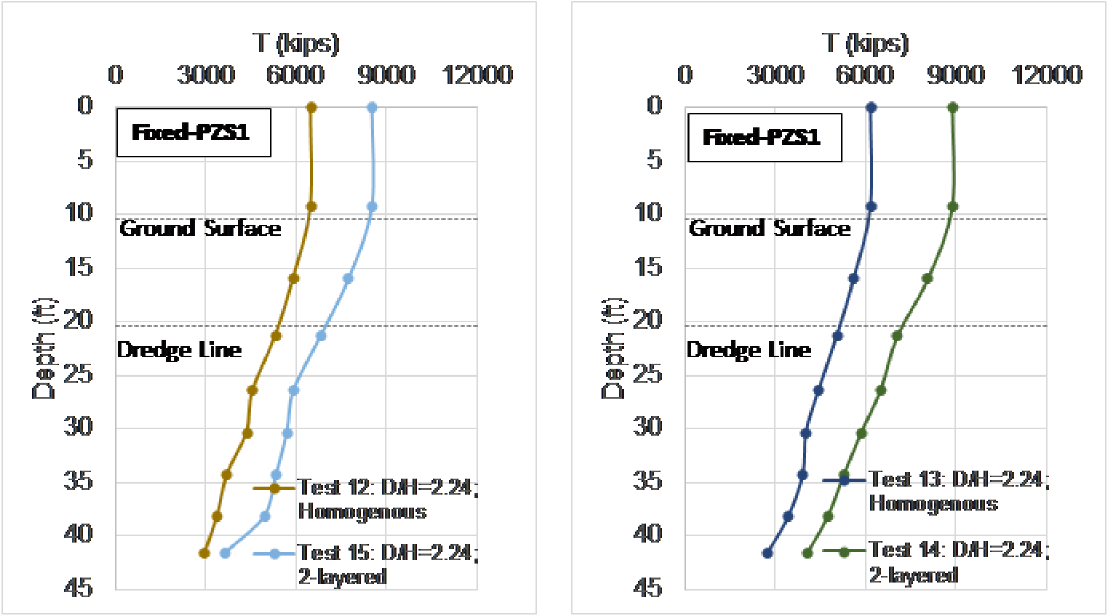

(a) (b)

Figure 31: Increased axial resistance of the sheet pile wall PZS1 in the profile PR2 compared to that in the profile PR1 with CRP : (a) CPR=7.87×10^{-4} in/s; and (b) CPR=7.87×10^{-5} in/s for d/h = 2.24

Task 3 - Centrifuge Results

- For uniform layers: pile wall is in medium dense sand with relative density D_r = 63%. (PR1)

- For layered sand : pile tip is embedded in very dense sand (D_r = 85%) underlaying a medium dense sand. (PR2)

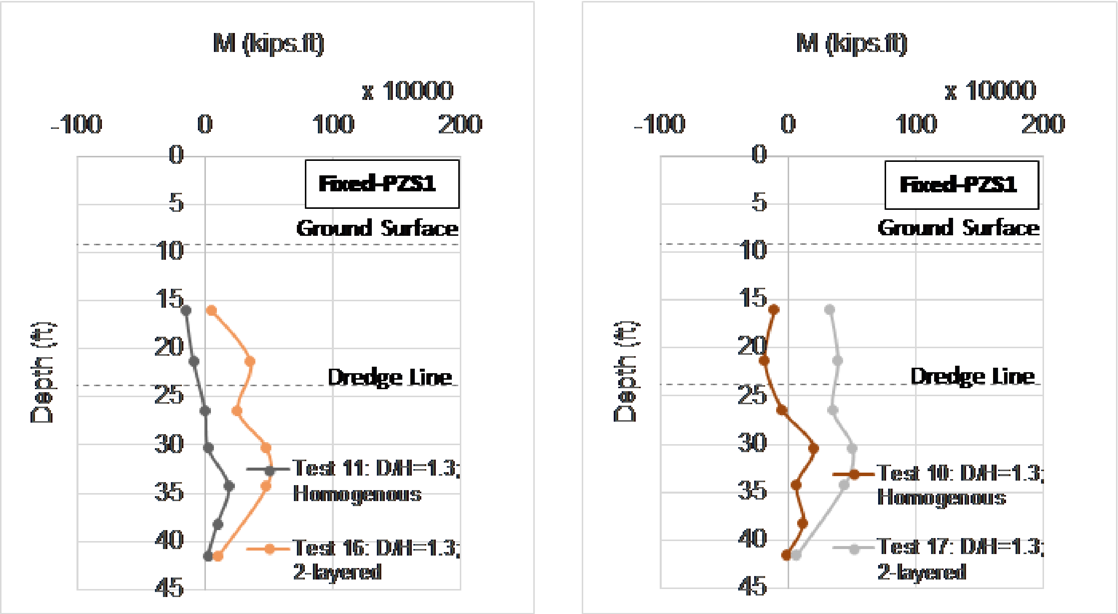

Figure 32: Bending moment profiles of the sheet pile wall PZS1 in the profile PR2 compared to that in the profile PR1 (a) CPR=7.87×10^{-4} in/s; and (b) CPR=7.87×10^{-5} in/s

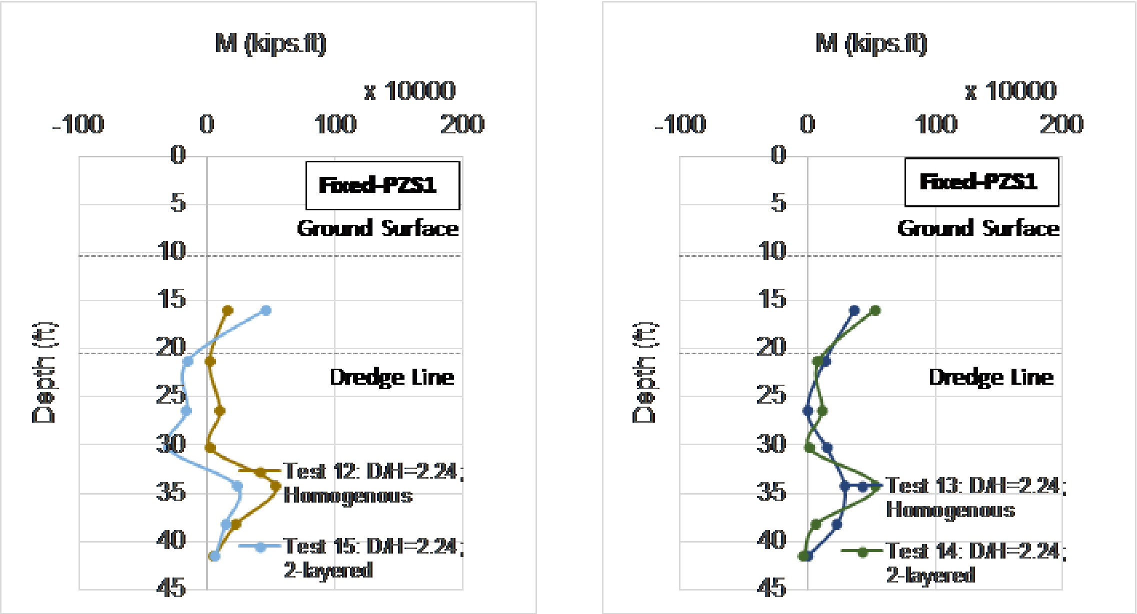

Figure 33. Bending moment profiles of the sheet pile wall PZS1 in the profile PR4 compared to that in the profile PR3: (a) CPR=7.87×10^{-4} in/s; and (b) CPR=7.87×10^{-5} in/s

Task 3 - Centrifuge Results

- Effects of depth of penetration (D) and unsupported length (H) on the axial behavior and bearing resistance of the sheet pile walls are investigated
- Two different penetration depth to retained soil height ratios (D/H) of 1.3 and 2.24 were considered.

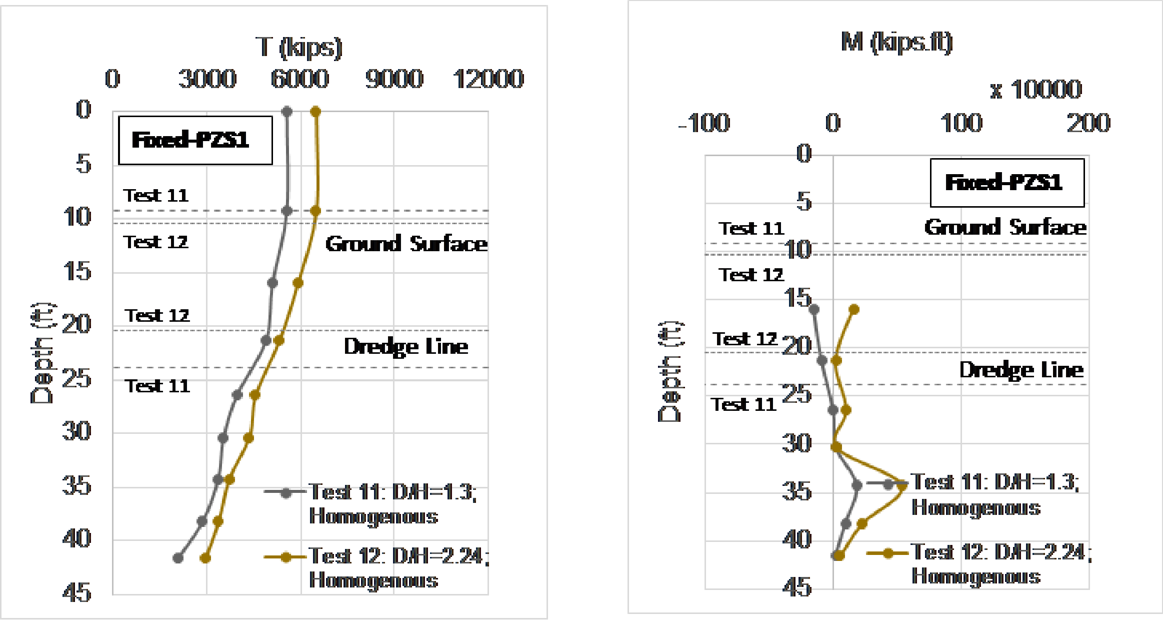

(a) (b)

Figure 34: Influence of relative retained heights of soil on the (a) axial resistance and (b) bending moment profiles in sheet pile wall section PZS1.

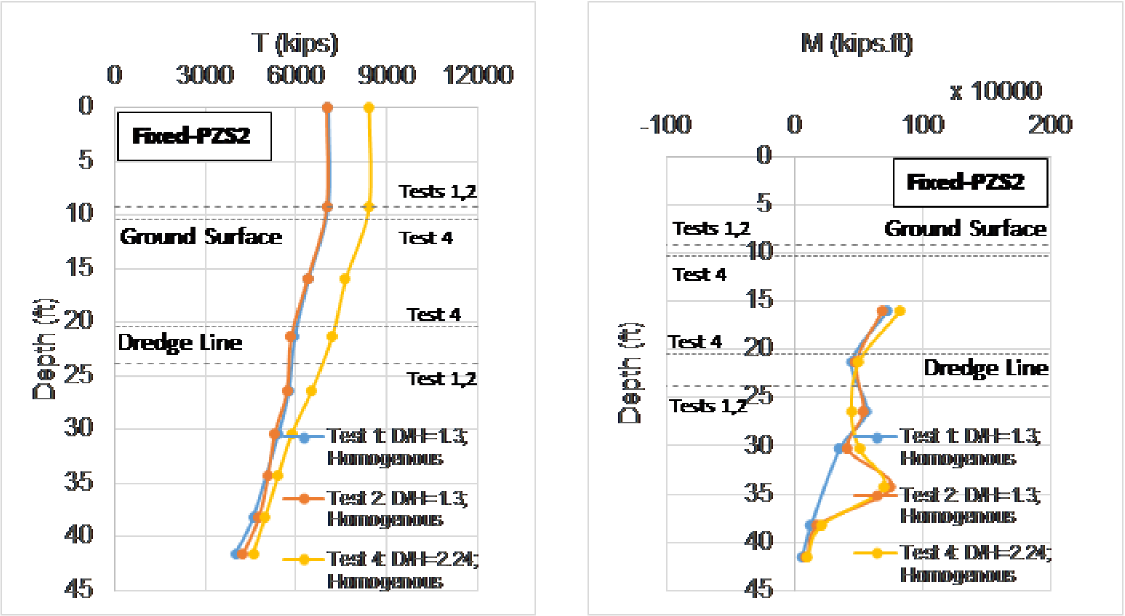

(a) (b)

Figure 35: Influence of relative retained heights of soil on the (a) axial resistance and (b) bending moment profiles in sheet pile wall section PZS2.

Summary of centrifuge testing

- The behavior of axially loaded sheet pile walls was investigated through centrifuge testing.
- A strain-hardening type axial load-displacement behavior was observed (attributed to soil plugging).
- Emplacement of pile wall tip in denser sand increased axial resistance, more so for d/h = 2.24 than d/h =1.3 (attributed to greater compaction due to longer driving time).
- Increasing sheet pile stiffness (cross-section area) improves the load bearing capacity.
- Rate effects observed are minimal due to absence of pore pressure and damping forces which is consistent with existing literature on pile walls in dry sands (any discrepancy can be attributed to instrumentation error) .

Task 4 – Validation & design equations

Numerical model translation of the prototype scale centrifuge soil-pile test

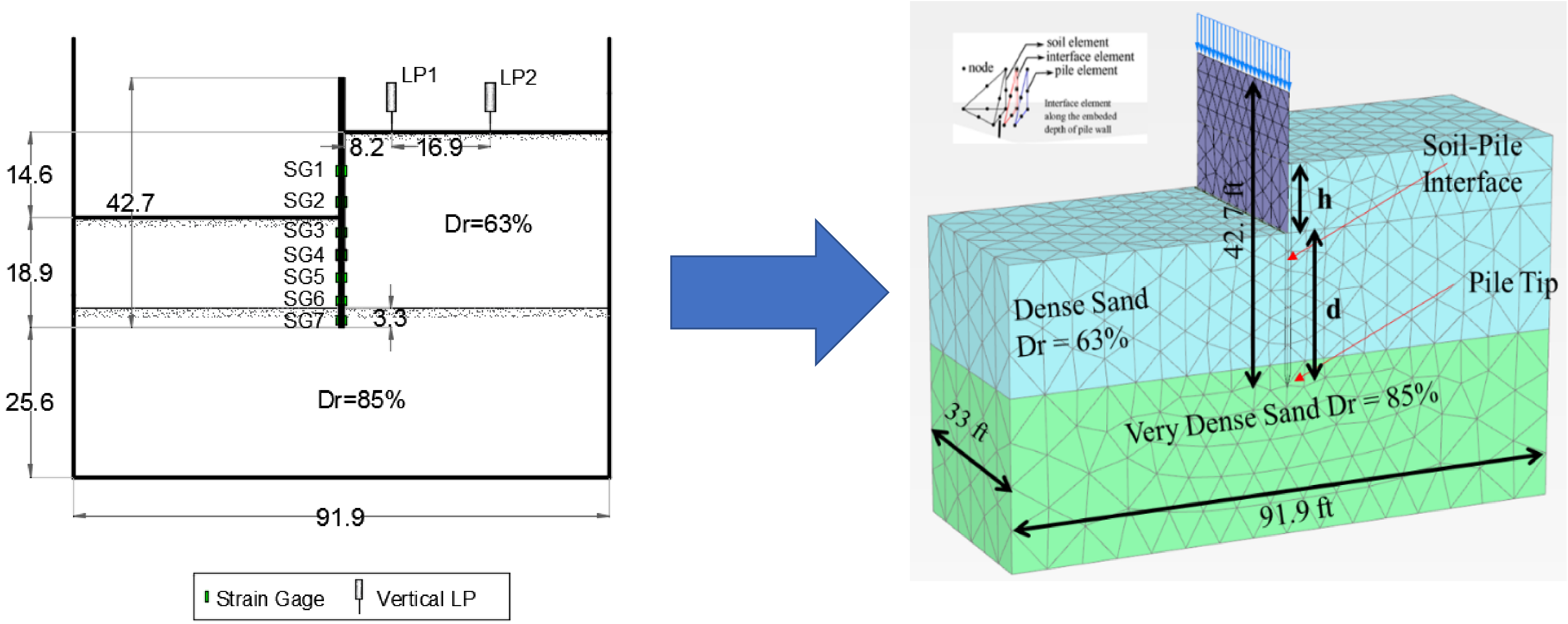

Fig 36: The centrifuge test setup for the scale model and the equivalent numerical model

Task 4 – Load displacement plots

Comparison of the experimentally observed and numerical calculated load curves

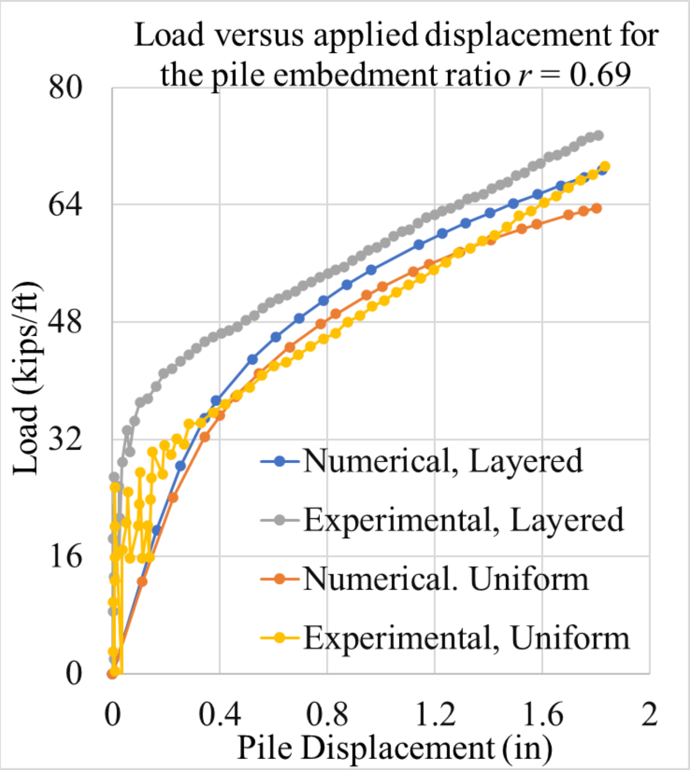

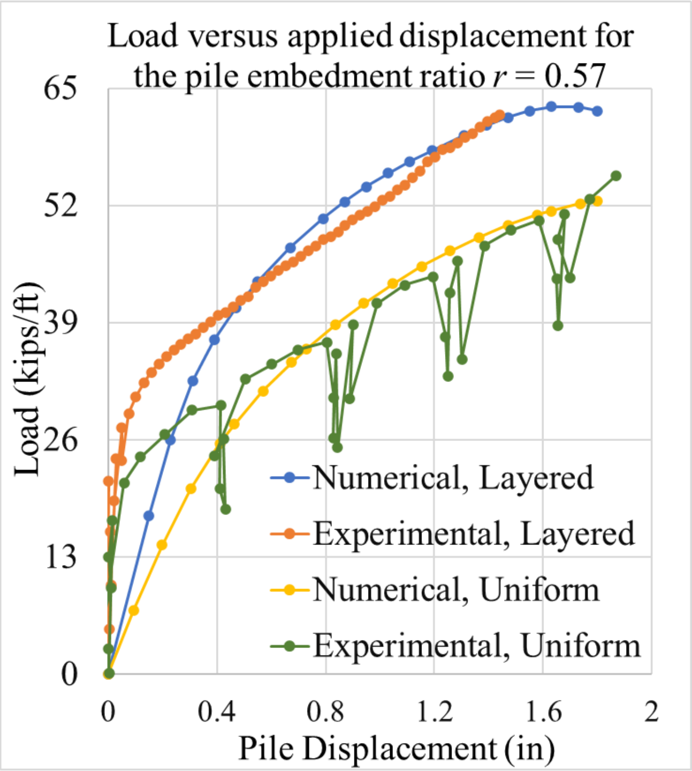

Figure 37: Plot of load versus vertical displacement from numerical model and centrifuge test for (left) embedment ratio r = 0.69 (right) embedment ratio r = 0.57

Task 4 – Parameter analysis

Modeling the influence of the identified design parameters on the bearing capacity using the new validated numerical model

Parameter	No. of Cases	No. of Pile Depths Considered	Total No. of Simulations
Density	10	10 (15 – 22.5 ft)	100
Soil friction angle	10	10 (15 – 22.5 ft)	100
Tip Resistance	10	10 (15 – 22.5 ft)	100
Head Boundary	20	10 (15 – 22.5 ft)	200

- The base simulations are conducted using uniform sand profile for 10 embedment ratios in 3 different sands (density and friction angle)
- The effect of tip resistance is modeled using soil layering: the tip of the pile wall is embedded in very dense sand which is overlaid by different sand layer
- The influence of the head boundary conditions is studied by comparing a fixed and free head condition in identical pile-soil systems (both layered and uniform).

Task 4 – Soil internal friction

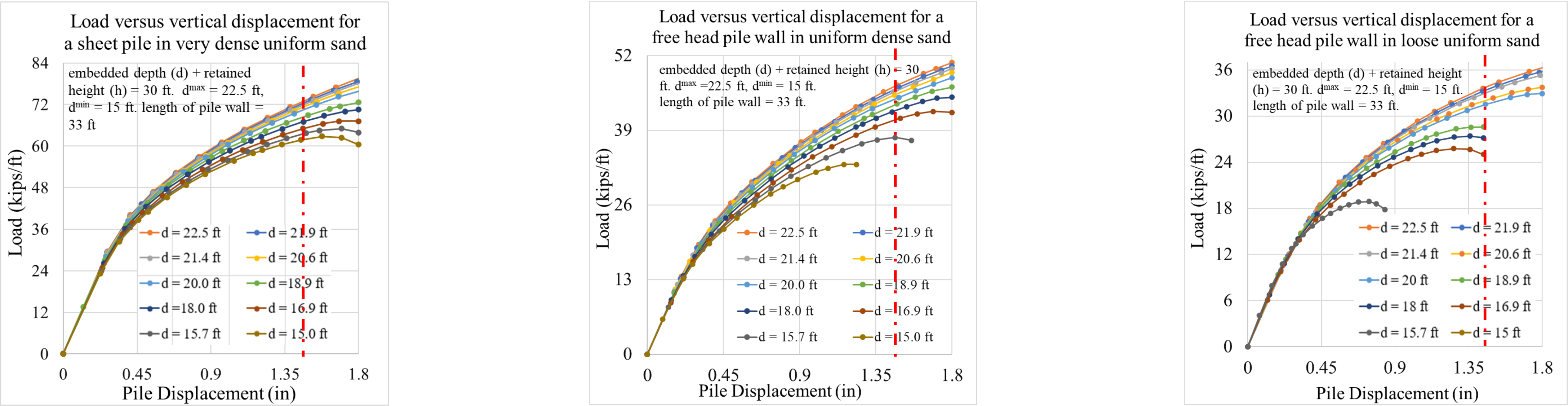

Figure 38: Plots of applied load versus displacement (left) D_r =85 % (ϕ = 35°), (center) D_r = 63 % (ϕ = 32°), and (right) D_r = 40 % (ϕ = 27°)

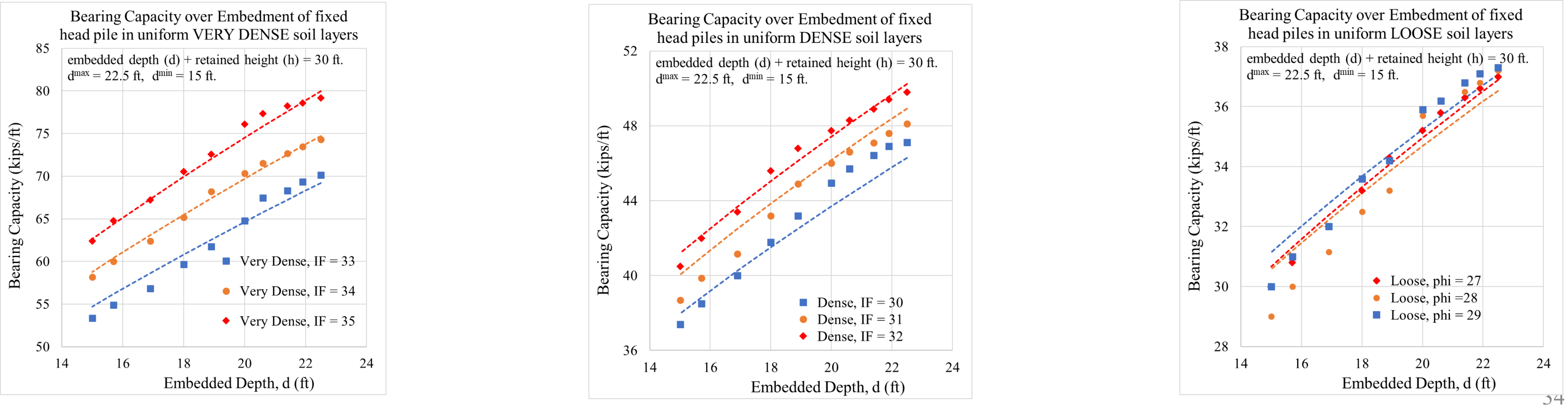

Figure 39: Plot comparing the bearing capacity over the embedment for <u>different soil densities</u>

Task 4 – Soil internal friction

$$Q_{ult} = ((d+h)/d)^{0.8421} * (\tan\phi) * d^{k}\ kips/ft,$$

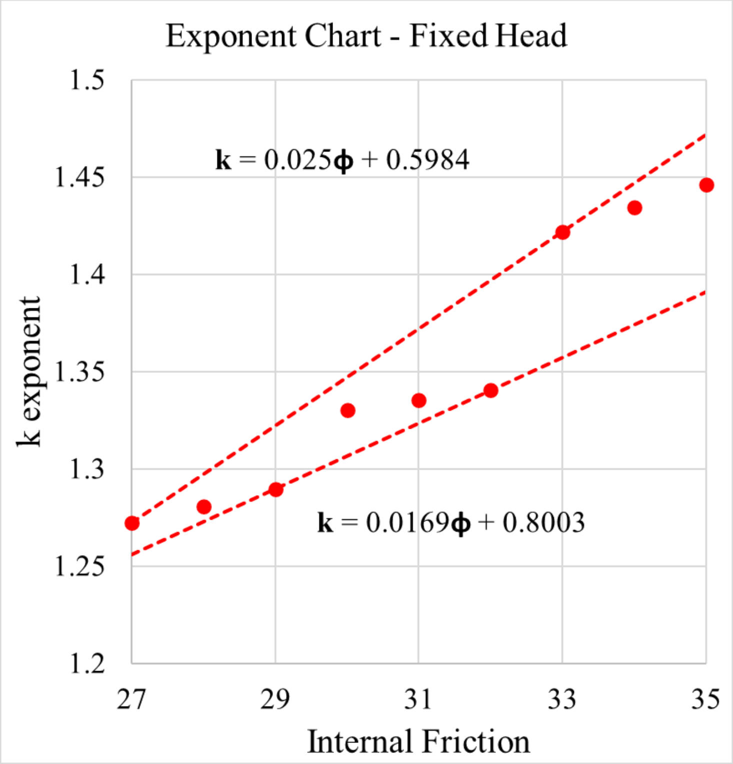

Figure 40: Plot comparing the bearing capacity over the embedment for different soil densities

$\boldsymbol{k} = 0.0169\boldsymbol{\phi} + 0.8003,$

$\boldsymbol{k} = 0.025\boldsymbol{\phi} + 0.5984,$

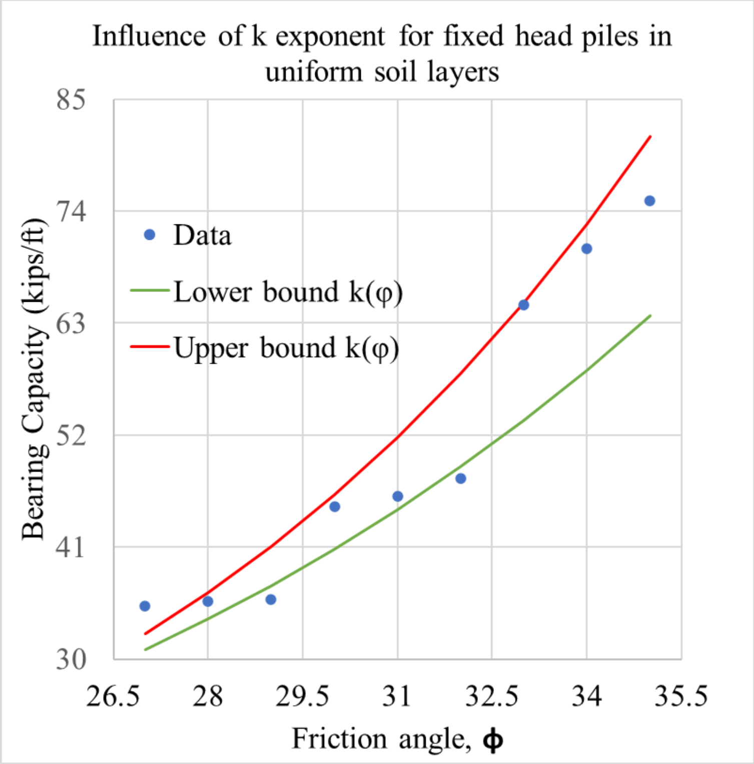

Figure 41: Comparison of the design equation for fixed head pile in uniform soil to the numerical data

Task 4 – Soil density

$$Q_{ult} = \frac{\gamma'}{\gamma_0}((d+h)/d)^{0.8421} * (tan\phi) * d^{k} kips/ft,$$

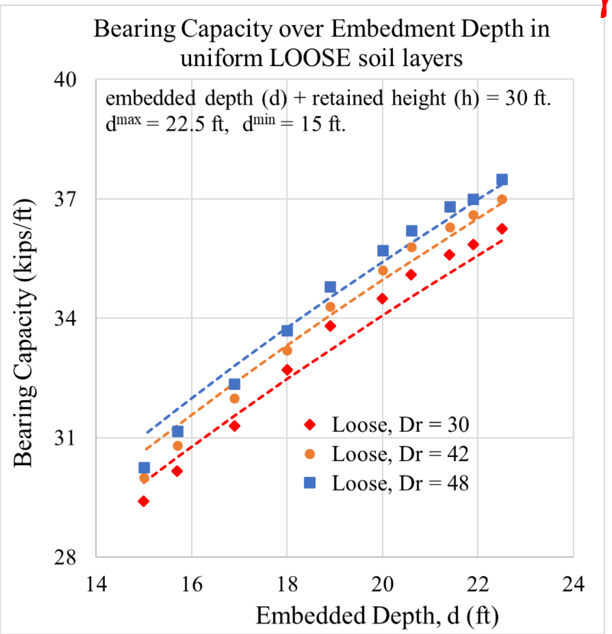

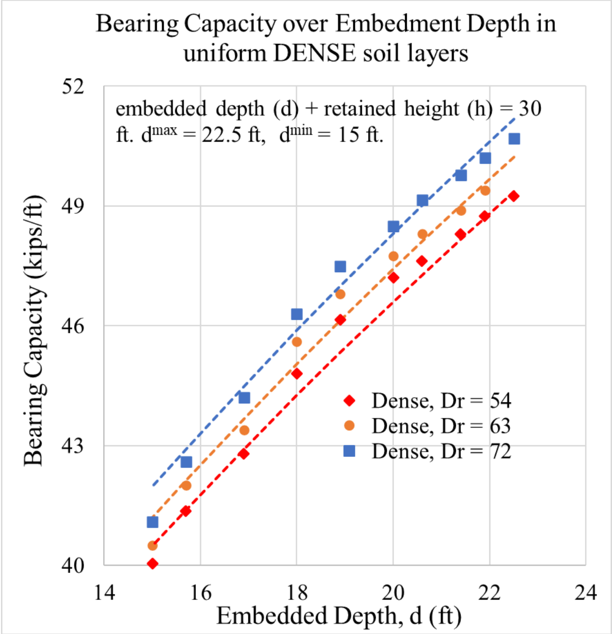

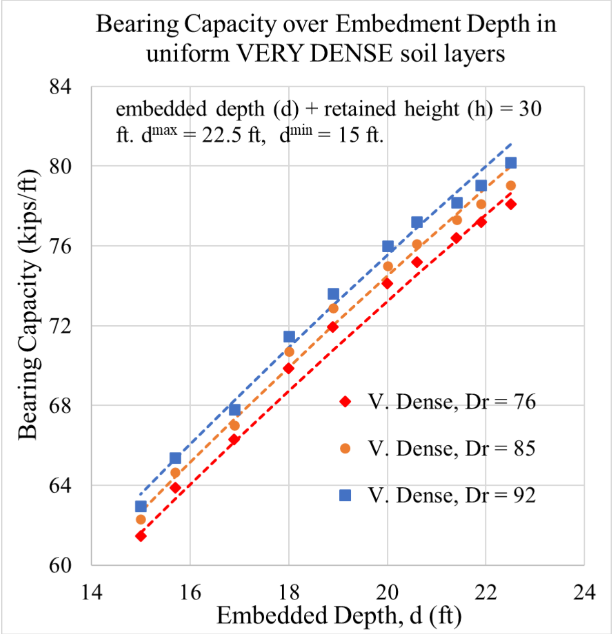

Figure 42: Plots of bearing capacity over embedment for (left) ϕ = 27°, (center) ϕ = 32°, and (right) ϕ = 35° considering different soil unit weights

Table 1 – Soil Unit Weights and Relative Density for simulations

Soil Classification	Internal Friction ϕ	Unit Weights (pcf) γ'	Relative Density D_r (%)
Loose	27	94.90, **97.35**, 98.59	30, **42**, 48
Dense	32	99.83, **101.7**, 103.5	54, **63**, 72
Very Dense	35	104.4, **106.2**, 107.7	76, **85**, 92

Task 4 – Soil layering

Modeling the influence of soil layering / tip resistance / end bearing

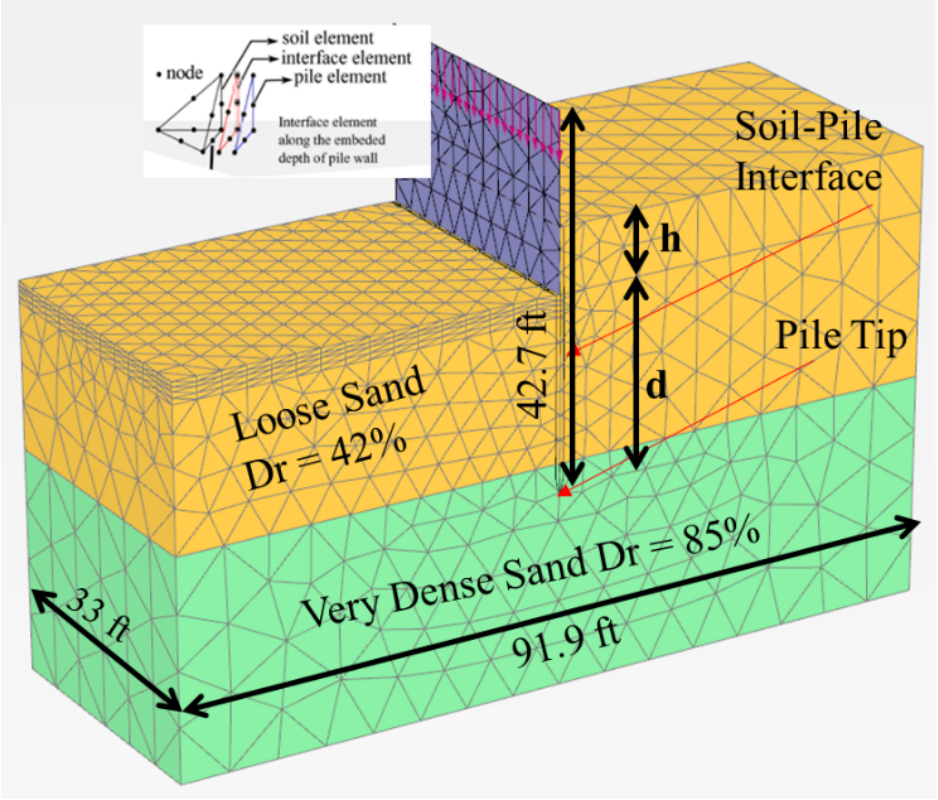

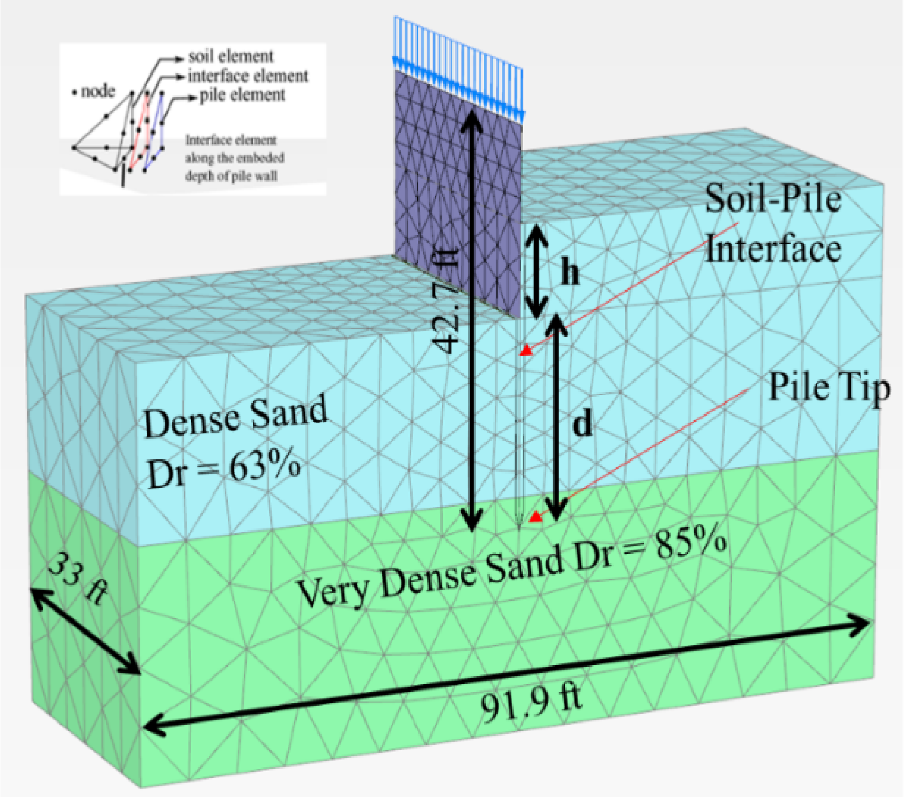

Figure 43: An illustration of the (left) layered soil profile A (loose sand over very dense sand) and (right) layered soil profile B (dense sand over very dense sand).

Task 4 - Soil layering

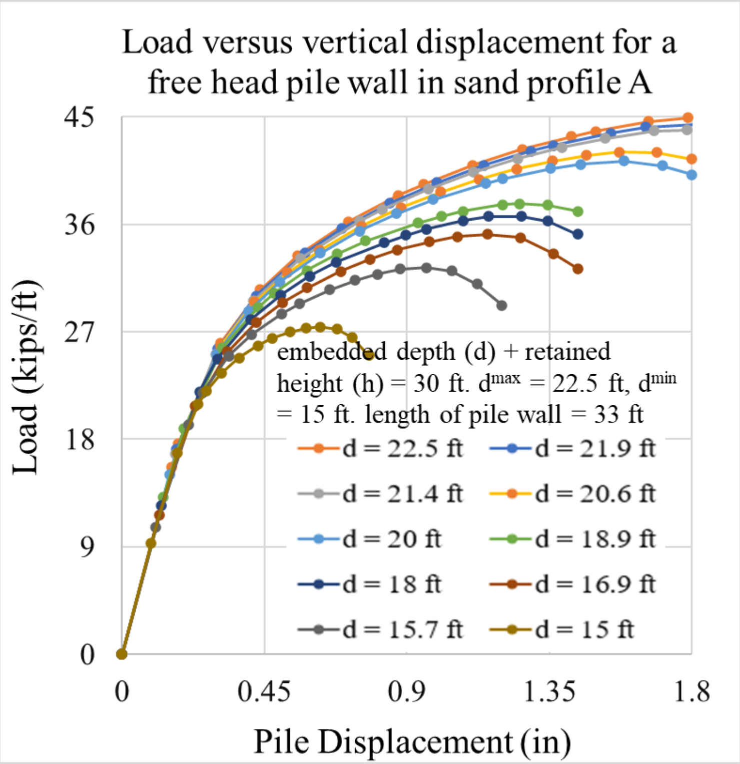

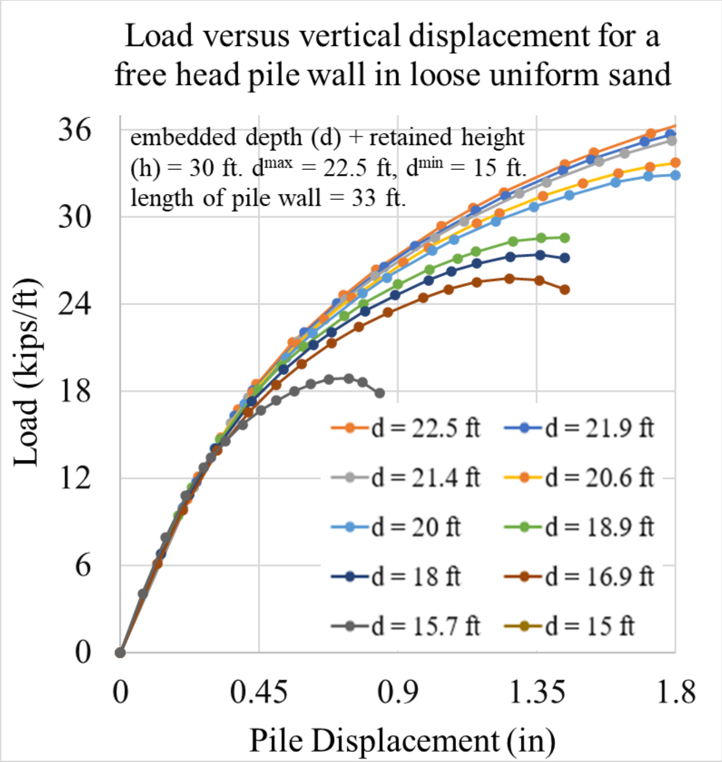

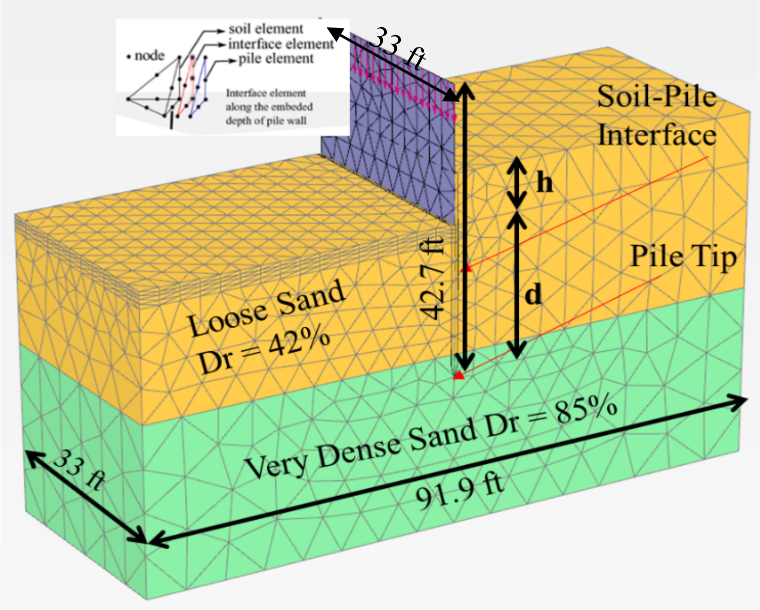

Figure 44: Plot of load versus displacement for a sheet pile embedded in (left) uniform loose soil and (right) layered profile A (loose sand over very dense sand)

Task 4 - Soil layering

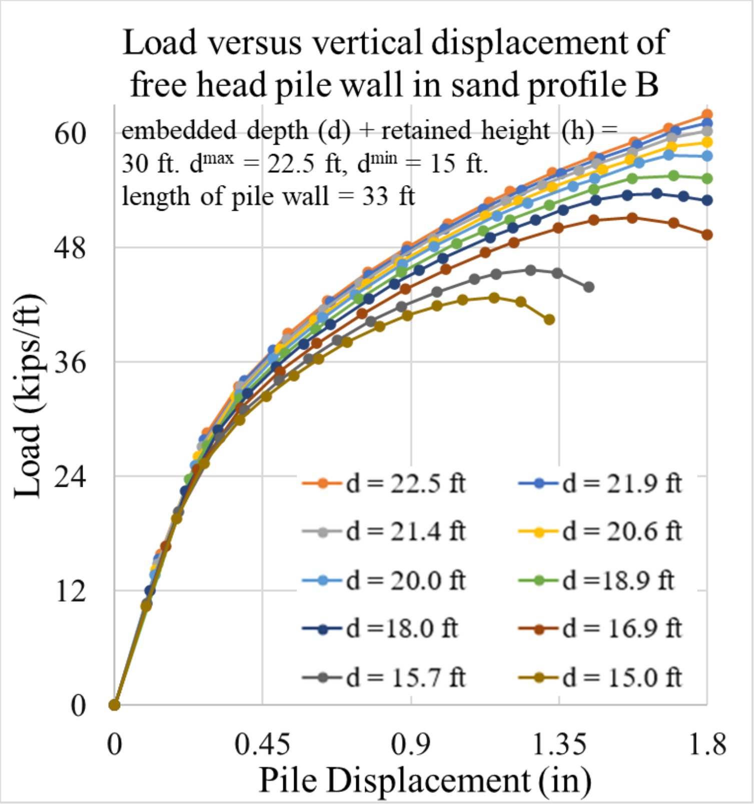

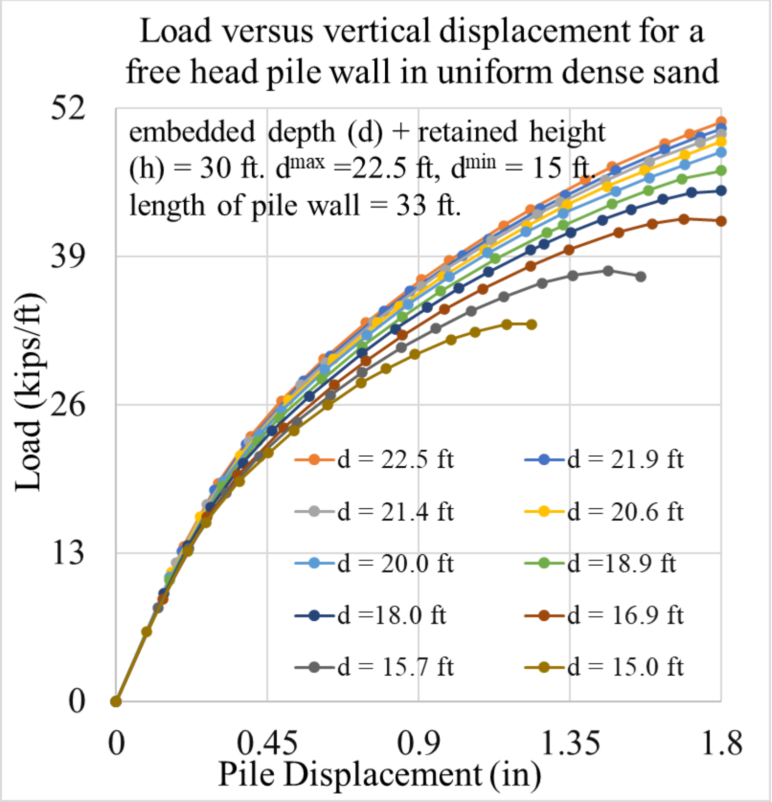

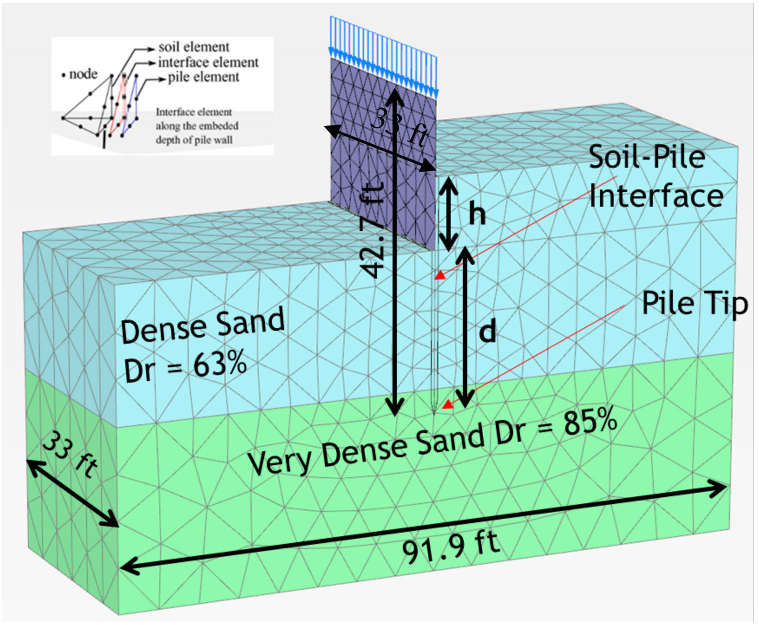

Figure 45: Plot of load versus displacement for a sheet pile embedded in (left) uniform dense soil and (right) layered profile B (dense sand over very dense sand)

Task 4 - Soil layering

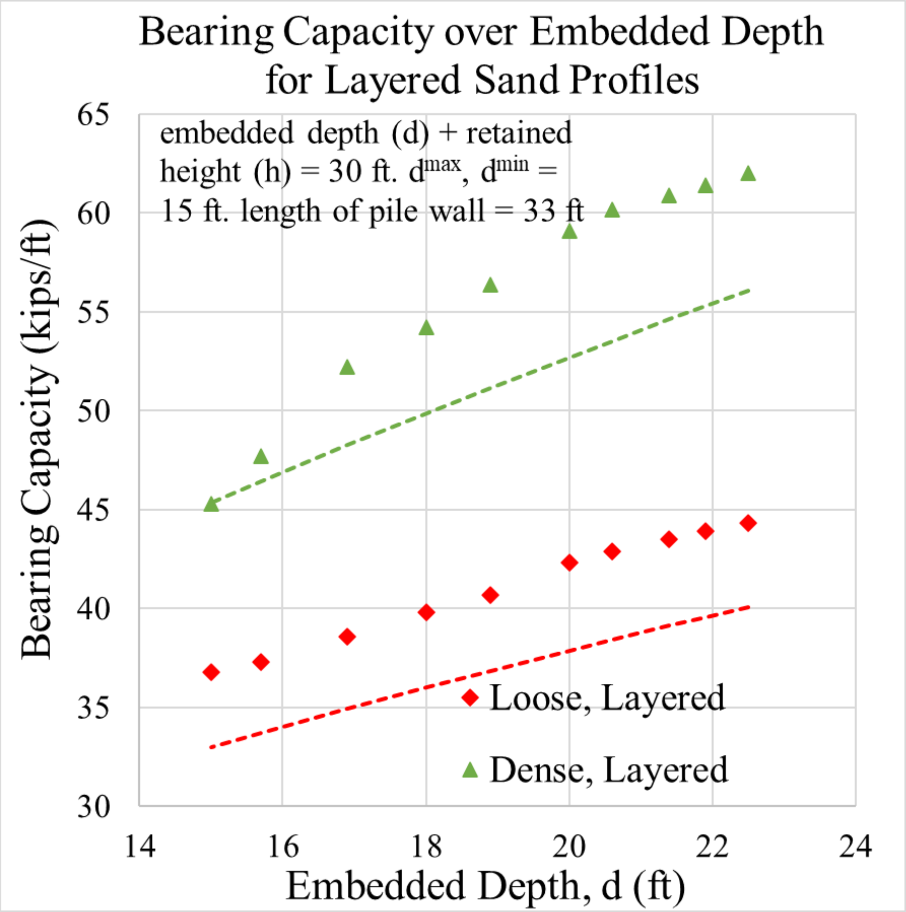

Figure 46: Plot comparing the bearing capacity over the embedment for layered and uniform soil profiles

$$Q_{ult} = \frac{\gamma'}{\gamma_0}((d+h)/d)^{0.8421} * (tan\phi) * d^{(k1+k2)/2}\ kips/ft$$

Note: these equations are valid for the 33 ft long sheet pile in the model.

Task 4 – Head fixity

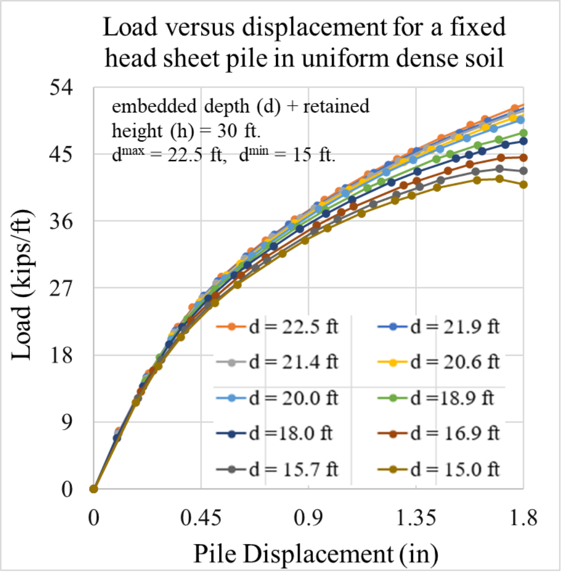

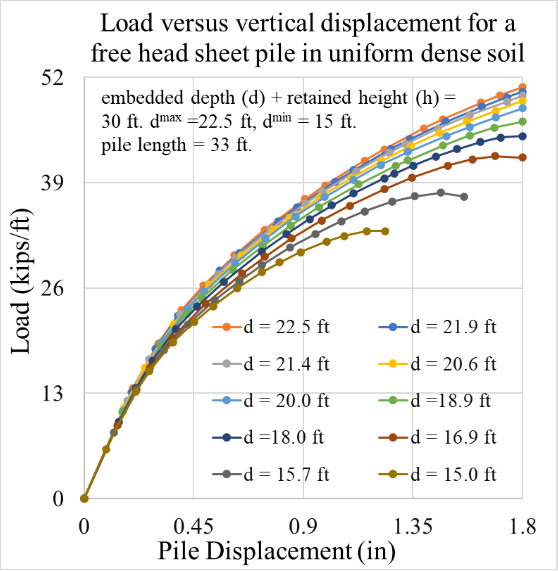

Figure 47: Plot of the load versus applied displacement for (left) a fixed head pile and (right) free head pile in **uniform dense** sand

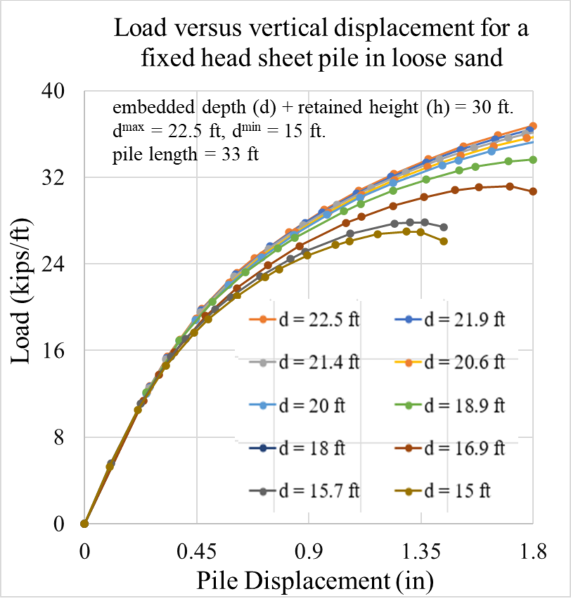

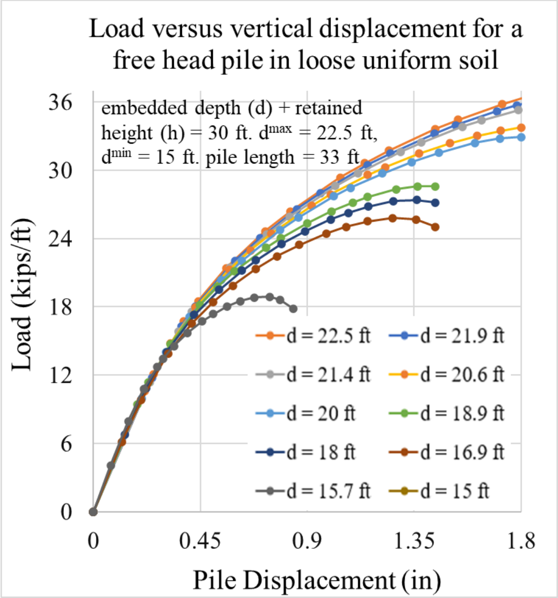

Figure 48: Plot of the load versus applied displacement for (left) a fixed head pile and (right) free head pile different embedment ratios in **uniform loose** sand

Task 4 - Head Fixity

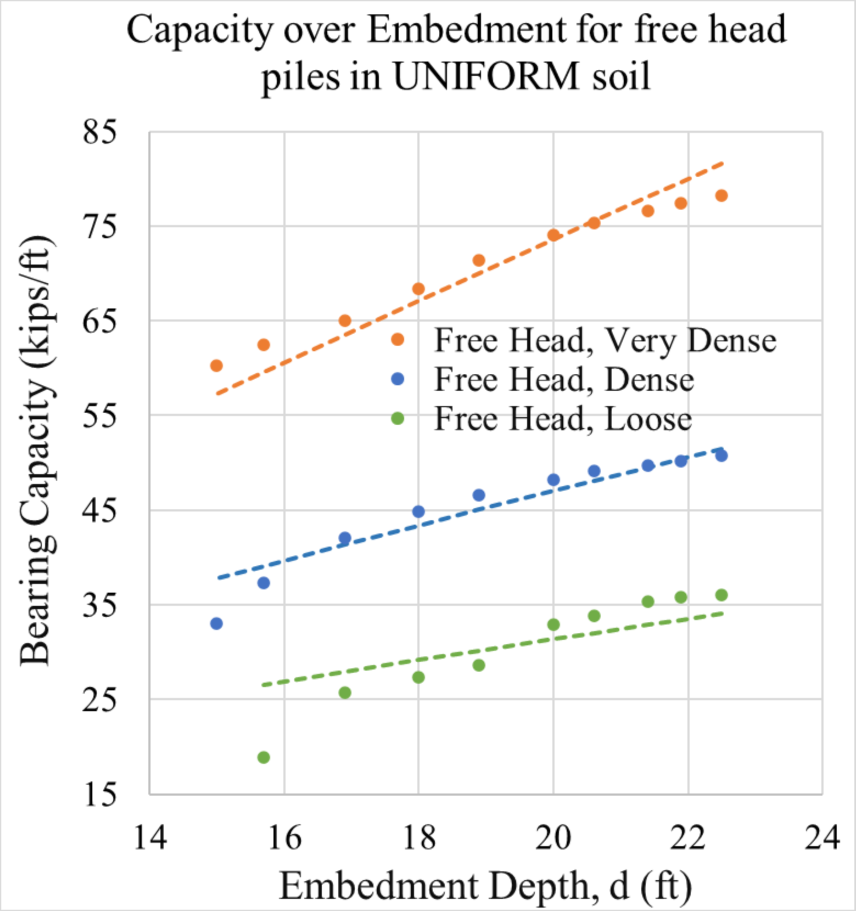

Figure 49: Plot comparing the bearing capacity over embedment ratio for different head boundary condition in uniform soil profiles

$$Q_{ult} = \frac{\gamma'}{\gamma_0}((d+h)/d)^{0.6} * (tan\phi) * d^k \ kips/ft,$$

Note: these equations are valid for the 33 ft long sheet pile in the model.

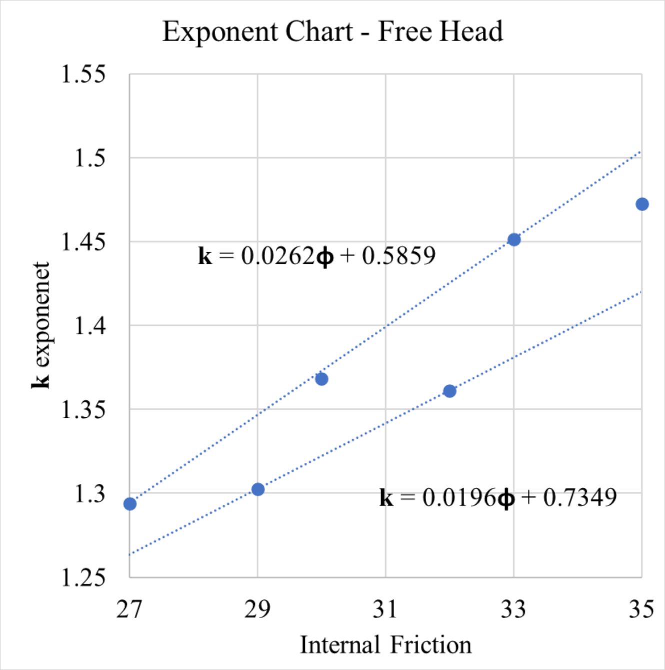

Figure 49: Plot of the exponent variation over the internal friction of the soil

Project Summary

- Sheet pile-soil systems exhibit strong "hardening" behavior under axial loading due to soil plugging
- There is a simple linear relationship between bearing and soil D_r
- End bearing resistance dominates the vertical bearing resistance for all scenarios considered
- Head fixity becomes important when $d/h < 1.67$ and $D_r < 60\ \%$

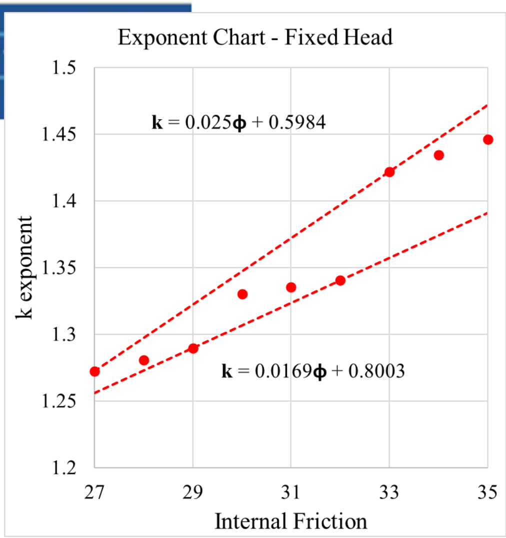

Project Summary

- The general equation of vertical bearing capacity

$$Q_{ult} = ((d+h)/d)^{0.8421} * (tan\phi) * \mathrm{d}^{k}\ kips/ft$$

- Effect of relative density can be represented by linear multiplier

$\frac{\gamma'}{\gamma_0}$, γ_0 = 97.3, 101.7, 106.2 pcf for loose, dense and very dense sand

- For soil layering the design equation can be modified as

$$Q_{ult} = \frac{\gamma'}{\gamma_0}((d+h)/d)^{0.8421} * (tan\phi) * \mathrm{d}^{(k1+k2)/2}\ kips/ft$$

- For a fixed head

$$Q_{ult} = \frac{\gamma'}{\gamma_0}((d+h)/d)^{0.6} * (tan\phi) * \mathrm{d}^{k}\ kips/ft,$$

Future work – Field load test

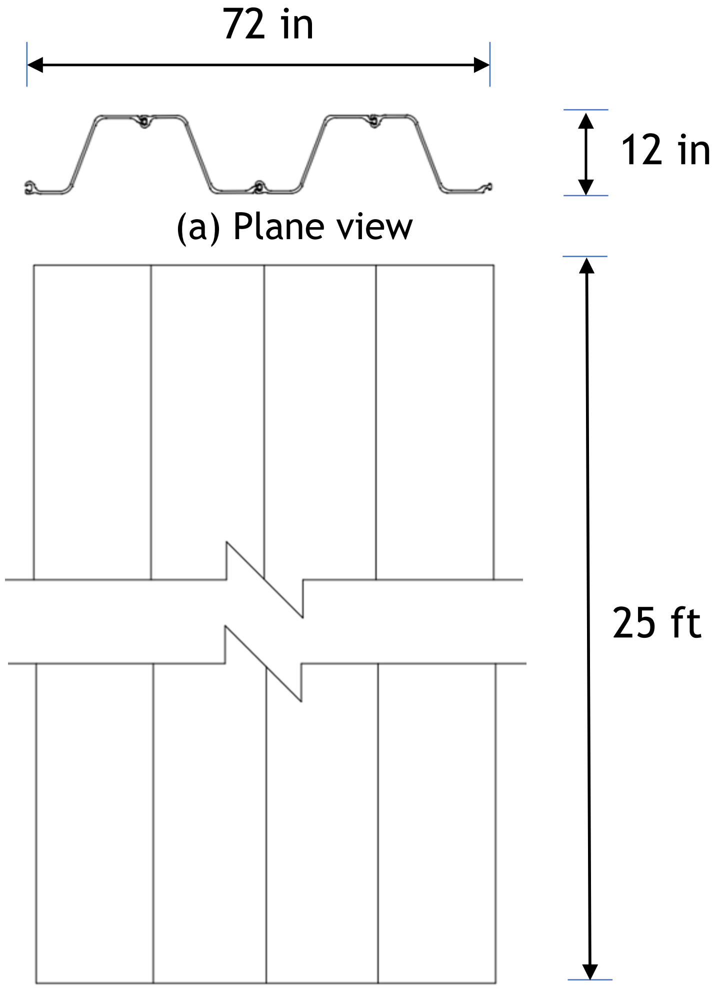

Figure: Grouped sheet piles

- Four PZ 27 sections, e.g., a sheet pile wall of length 72 in
- Length of each sheet pile: 25 ft

Steel sheet pile

Installation

Static load test

APPLIED FOUNDATION TESTING (AFT) Specialty Geotechnical Services provides reaction beams, tie-down beams, load cells, hydraulic jacks, and strain gages.

Site location - Keystone Heights

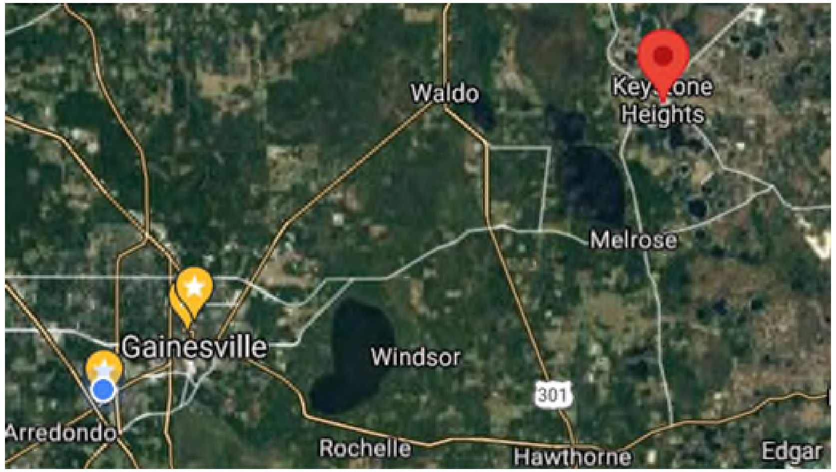

Recommendations

- Conduct field testing of the sheet pile to further validate the bearing equations
- Use of lower bound of the ‘k’ exponent to maintain a safety factor
- Anchoring the pile head is recommended for low soil density or low embedment ratio

Acknowledgements

We thank the FDOT for funding this research project.

We are grateful to Juan Castellanos, David Horhota, Rodrigo Herrera and Larry Jones for their support and insightful discussions on this project.

We thank Don Robertson at AFT for his help in drafting the field testing protocol.

Thank you!

Questions?